Mass Transfer in Agitated Liquid-Solid Systems

By

Shinji NAGATA*, Iwao YAMAGUCHI*, Seizo YABUTA*
and Makoto HARADA*

(Received October 28, 1959)

The authors performed experiments on the solution of solid particles in agitated liquids in a series of geometrically similar agitators. A great variety of solid particles, including several kinds of spherical crystals, whose particle size, shape and density varied over a wide range were used as the solid samples. Pure water, dilute hydrogen chloride and aqueous solutions of gelatine, polyvinyl alcohol, sucrose and glycerine of various concentrations were used as the liquids.

Several methods for determining the rate of solution of solid particles were considered, and the analysis of the data was performed in terms of the mass transfer coefficient.

As for the experimental results on the agitation process, it was found that the physical properties of the solid particles, *i. e.*, the difference in density between the liquid and the solid, the size and shape of the particles, as well as the viscosity and the density of the liquid were important factors controlling the rate of mass transfer.

Between the agitator speeds of N_f and N_a all the data were correlated by the following dimensionless equations.

For solid particles with an unknown surface shape factor,

$$\left(\frac{K'D}{D_f}\right) = 3.60\times10^{12}\left(\frac{D^2n}{\nu}\right)^{p}\left(\frac{\nu}{D_f}\right)^{q}\left(\frac{D_f{}^2}{D^3g}\right)^{0.627}\left(\frac{d_p}{D}\right)^{3.08}\left(\frac{\rho_s-\rho_l}{\rho_l}\right)^{-2.82}$$

and for solid particles with a known surface shape factor,

$$\left(\frac{KD}{D_f}\right) = 3.60\times10^{12}\left(\frac{D^2n}{\nu}\right)^{p}\left(\frac{\nu}{D_f}\right)^{q}\left(\frac{D_f{}^2}{D^3g}\right)^{0.627}\left(\frac{d_p}{D}\right)^{3.08}\left(\frac{\rho_s-\rho_l}{\rho_l}\right)^{-2.82}\left(\frac{\Phi_s}{\pi}\right)^{-1}$$

where

$$p = 0.0802\left(\frac{D^3g}{\nu^2}\right)^{0.0772}\{\log(\Delta+0.043)+1.35\}10^{-13\,5\delta}$$

$$q = -14.4\delta+1.84\Delta^{0.116}$$

These equations represent the general correlation of the variables involved in determining the magnitude of the rate of mass transfer in agitated liquid-solid systems, and are used to estimate the mass transfer rate for any liquid-solid combination in a series of geometrically similar vessels and impellers.

* Department of Chemical Engineering.

1. Experimental Conditions and Procedures.

(a) Experimetal Apparatus.

As the agitation vessel, the authors used a series of dimensionally similar cylindrical vessels with flat bottoms. Symbols representing the dimensions of the various parts of the agitation apparatus are shown in **Fig. 1.**

A glass cylinder of diameter $D=10$ cm was the one mainly used in the experiments, and the liquid depth was always chosen equal to the vessel diameter, *i.e.*, $H_l=D=10$ cm. The impeller used was a four-blade paddle type of diameter $d=5$ cm, width of blade $b=1.5$ cm, blade angle $\theta=75°$. The elevation of the impeller was $H_p=4$ cm.

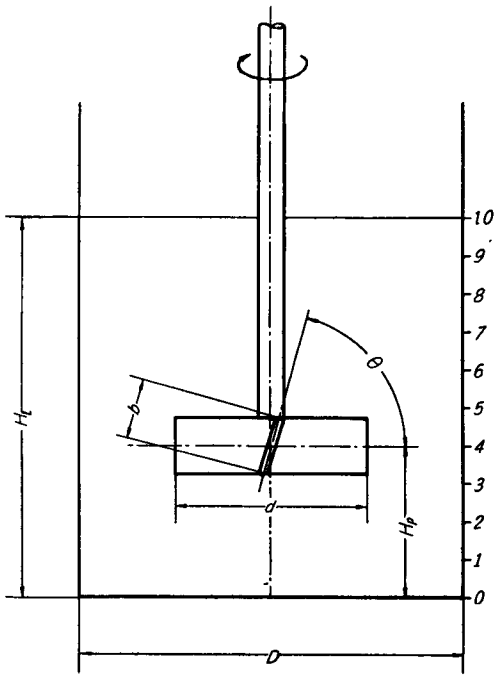

Fig. 1. Agitation apparatus.

For the purpose of making clear the effect of the vessel diameter, a series of geometrically similar vessels made of plastic with varying diameters ($D=10$, 15, 20 and 30 cm) were used. The impeller used was a four-blade paddle type of diameter $d=0.5D$, width of blade $b=0.1D$, blade angle $\theta=90°$ and elevation of the impeller $H_p=0.4D$. Liquid depth $H_l=D$.

In some experiments other impellers were used with $b=0.2D$ and $\theta=90°$, and $b=0.1D$ and $\theta=45°$.

An electrode made of two platinum plates (1×1 cm wide, 1.5 mm distance) was set in the agitated liquid in order to measure directly the electric conductivity of the agitated liquid. Thus the change in concentration with elapsed time was measured.

(b) Materials Used in the Experiments.

It is advisable to use solid particles whose size is uniform and whose solubility is low, *i.e.*, the rate of solution is low. The higher the electric conductivity of the solution, the smaller the experimental error. The physical properties of the crystals used are shown in **Table 1** and **2.**

Ordinary Zn powder of granular shape was used. The details of the preliminary treatment before use have been stated in a previous paper[1]. Spherical $AgNO_3$

Table 1. Conditions of solid particles used and the observed values of p.

Notation / Unit	Shape	Particle size range [mesh]	Amount of solid used W [g/785 cc]	Number of particles used n [—]	Particle diameter d_p [mm]	Exponent p_1 [—]	Exponent p_2 [—]
Zn (ρ_s=6.95)	granular	120~150	2.500	5.02×10^5	0.111	2.54	0.980
		100~120		2.98×10^5	0.132	2.42	0.970
		80~100		1.46×10^5	0.167	2.30	0.960
$AgNO_3$ (ρ_s=4.08)	spherical	28~35	1.000	2.50×10^3	0.572	1.51	0.740
		20~28		1.18×10^3	0.744	1.42	0.660
		16~20		4.95×10^2	0.982	1.34	0.620
		12~14		1.90×10^2	1.35	1.24	0.545
		10~12		1.00×10^2	1.67	1.18	0.498
$KMnO_4$ (ρ_s=2.66)	granular	60~100	1.000	6.14×10^4	0.227	1.59	0.710
		10~16		1.82×10^2	1.58	1.00	0.465
$K_2Cr_2O_7$ (ρ_s=2.63)	granular	60~100	2.000	1.38×10^5	0.220	1.53	0.690
		45~60		3.17×10^4	0.358	1.43	0.660
		28~45		1.04×10^4	0.519	1.39	0.625
		16~28		1.59×10^3	0.973	1.15	0.545
		10~16		5.75×10^2	1.36	1.10	0.490
NaCl (ρ_s=2.10)	spherical	28~35	2.000	5.02×10^3	0.566	1.21	0.592
		16~20		8.34×10^2	1.03	1.05	0.520
		12~14		3.69×10^2	1.35	0.988	0.475
		10~12		1.61×10^2	1.78	0.927	0.412
		8~10		7.75×10^2	2.27	0.878	0.387
NaCl (ρ_s=2.02)	cubic	10~12	2.000	1.96×10^2	1.69	0.923	0.412
NH_4NO_3 (ρ_s=1.65)	spherical	12~14	1.000	4.03×10^2	1.42	0.916	0.357
		10~12		2.58×10^2	1.65	0.886	0.336
		8~10		1.18×10^2	2.14	0.835	0.293
NH_4Cl (ρ_s=1.49)	granular	8~16	2.000	1.33×10^2	2.13	0.745	0.275
H_3BO_3 (ρ_s=1.47)	spherical	60~100	2.000	2.15×10^5	0.230	1.33	0.510
		45~60		6.58×10^4	0.341	1.17	0.490
		28~45		1.85×10^4	0.519	1.08	0.480
		16~28		6.54×10^3	0.737	1.02	0.440
	triclinic	28~45		1.50×10^4	0.557	1.13	0.490
		16~28		4.16×10^3	0.858	0.850	0.410
$CO(NH_2)_2$ (ρ_s=1.26)	spherical	16~20	1.000	1.73×10^3	0.957	0.776	0.275
		14~16		9.25×10^2	1.18	0.743	0.263
		10~12		3.21×10^2	1.68	0.683	0.225
		8~10		2.08×10^2	1.94	0.662	0.213
Phenylacetic acid (ρ_s=1.21)	plate	16~28	1.000	3.60×10^3	0.762	0.800	0.310
		10~16		1.63×10^3	0.990	0.750	0.275
Crotonic acid (ρ_s=1.16)	monoclinic (flat)	16~28	0.500	1.67×10^3	0.790	—	0.230
		10~16		2.26×10^2	1.54	—	0.160
	monoclinic (cubic)	28~45	0.300	5.20×10^3	0.456	0.680	0.250
		20~28	0.500	2.16×10^3	0.728	—	—
		16~28		1.57×10^3	0.805	0.730	0.230
		10~16		2.05×10^2	2.00	—	0.180

Table 2. Conditions of solid particles used.

Notation / Unit	Shape	Density ρ_s [g/cm³]	Particle size range [mesh]	Amount of particles used W [g]	Number of particles used n [−]	Particle diameter d_p [cm]	d_p/D [−]
$K_2Cr_2O_7$	granular	2.63	45~60	2.00	3.31×10^4	3.53×10^{-2}	3.53×10^{-3}
			28~45 / 16~28 *	6.75	3.28×10^4	5.30×10^{-2}	〃
			28~45 / 16~28 *	16.00	2.89×10^4	7.06×10^{-2}	〃
			16~28 / 10~16 *	54.00	3.32×10^4	1.06×10^{-1}	〃
NaCl	cubic	2.02	28~35	2.00	1.01×10^4	5.73×10^{-2}	5.73×10^{-3}
			20~28 / 16~20 *	6.75	1.00×10^4	8.60×10^{-2}	〃
			16~20 / 12~16 *	16.00	9.95×10^3	1.15×10^{-1}	〃
			10~12	54.00	1.00×10^4	1.72×10^{-1}	〃
H_3BO_3	spherical	1.47	80~100	3.00	5.00×10^5	1.95×10^{-2}	1.95×10^{-3}
			60~80 / 45~60 *	6.75	3.48×10^5	2.93×10^{-2}	〃
			45~60 / 35~45 *	8.00	1.78×10^5	3.90×10^{-2}	〃
			28~35	27.00	1.75×10^5	5.85×10^{-2}	〃

* Mixture

particles were prepared by the authors as follows. Silver nitrate crystals of reagent grade were melted in a porcelain evaporating-dish at a temperature of about 250°C. and were drawn into a glass pipette which was preheated to about 250°C. and then quickly ejected through 30 mesh wire-gauze into liquid CCl_4 at room temperature by means of compressed air.

Ordinary potassium permanganate and potassium bichromate were sifted before use. As for sodium chloride, both spherical and cubic crystals were used. The former were presented by the Nihon Senbai Kosha (Japan Monopoly Corporation). Ammonium nitrate and urea are both spherical and are commonly used as fertilizer. Ammonium chloride is also a chemical fertilizer whose shape is similar to that of rice. Both the spherical and the triclinic crystals of boric acid were used. Triclinic H_3BO_3 was prepared by recrystallization. Phenyl acetic acid crystals for chemical use were also recrystallized under agitation to the shape of a rhombic leaflets. Monoclinic crotonic acid was recrystallized three times.

As the mean diameter of the solid particle the "diameter equivalent to that of a sphere of equivalent weight, d_p," was adopted in this paper. This mean diameter d_p was proposed by R. H. Wilhelm, *et al.*[2] and is defined by the following relation.

$$d_p = \sqrt[3]{\frac{6}{\pi}\left(\frac{w}{n\rho_s}\right)} \qquad (1)$$

The value d_p can be determined by the total weight (w) and the number of particles (n), preferably about 500.

In order to clarify the effect of the vessel diameter, the authors adopted a series of geometrically similar vessels and impellers. In this case it would be reasonable to use solid particles whose diameter is proportional to the vessel diameter. In order to make the particle sizes geometrically similar, two different though nearly equal sizes were mixed in a suitable proportion to yield the desired size.

For example, if particles of average diameter d_m are required, and particles of slightly different diameter, d_1 and d_2 ($d_1 < d_m < d_2$), are to be mixed together, the weight ratio m of d_1 and d_2 should be given by the following relation,

$$m = \frac{d_1^3(d_2^3 - d_m^3)}{d_2^3(d_m^3 - d_1^3)} \qquad (2)$$

Pure water whose electric conductivity was lower than 1×10^{-6} mho was mainly used as the agitated liquid. For the experiment on the solution of Zn powders, dilute hydrochloric acid was used and the detailed conditions have been given in the previous report[1]. To investigate the effects of the viscosity and density of the liquid, aqueous gelatine and P.V.A. solutions of various concentrations, were used. Sucrose solution and glycerine were also used. The observed values of the concentration, density and viscosity of these aqueous solutions are shown in **Table 3.**

Table 3. Properties of the agitated liquid at 25°C.

Solution	Concentration [wt. %]	Density ρ_l [g/cm^3]	Viscosity μ [c.p.]
H_2O	—	1.00	0.895
Gelatine/H_2O	2.00	〃	1.62
〃	4.00	〃	4.04
〃	6.00	〃	5.59
P.V.A./H_2O	1.50	〃	2.90
〃	2.00	〃	4.47
〃	2.50	〃	5.50
Glycerine/H_2O	25.0	1.06	1.68
Sucrose/H_2O	15.0	1.06	1.29
〃	30.0	1.13	2.30

Though the solutions of gelatine and P.V.A. are pseudo-plastic in nature, these solutions are adopted, because it is very difficult to prepare normal liquids with

different viscosities having equal density and solubility of the salt as compared with water. However, as a result of measurement of the viscosity under various pressures with Bingham and Jackson's viscometer[3], it was found that the deviation from a normal liquid was negligible in the range of concentration covered by the present experiments (refer to **Fig. 2**).

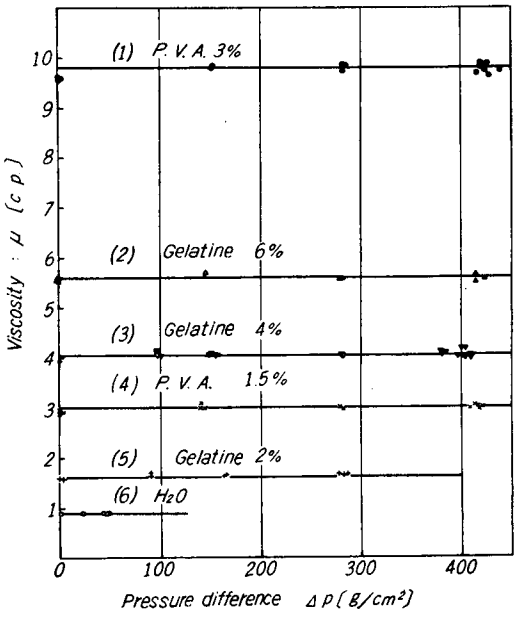

Fig. 2. Observed values of the liquid viscosity by Bingham and Jackson viscometer at different pressures.

(c) Experimental Procedures.

A definite quantity of liquid (785 cc for the vessel of $D=10$ cm) was charged in the agitation vessel and the temperature of the system was adjusted to 25.0 ± 0.1°C. constant for most runs. After a steady state of agitation was attained, a weighed amount of solid particles (ordinarily 2.00 g for the vessel of 10 cm, and an amount proportional to the liquid volume for the vessels of different size) was quickly introduced and a stopwatch started simultaneously. The change in electric conductivity and the corresponding time elapsed were measured.

The observed values were plotted on section paper referring to the electric conductivity—concentration chart which was prepared in advance from the observed values of electric conductivity using standard solutions of known concentration.

Experimental procedures and methods of estimating the rate of solution of Zn powders were explained in the previous paper[1].

2. Method for the Determination of the Rate of Solution of the Solid Particles and the Mass Transfer Coefficient.

The following equation based on Fick's law may be used as a basic equation for the quantitative analysis of the solution processes. The rate of solution of solid particles per unit volume is,

$$\frac{R}{V}=-\frac{dW}{Vd\theta}=K\frac{A}{V}(C_s-C) \qquad (3)$$

where R ($\equiv -dW/d\theta$) is the total rate of solution in the vessel. Various methods may be applicable to calculate the rate of solution by use of Eq. (3).

2. 1. Determination of the Rate of Solution.

(a) Hixson-Crowell's Method (Cube root law).

Since the following substitutions may be made,

$$A = \alpha_w W^{2/3}, \quad C_s = W_s/V, \quad \text{and} \quad C = (W_0 - W)/V,$$

Eq. (3) when integrated takes the following form, *i.e.*, Hixson-Crowell's Cube root law.

$$K\alpha_w\theta = \frac{V}{m^{2/3}}\left\{\sqrt{3}\tan^{-1}\frac{2\sqrt{3}\,m^{1/3}(W_0^{1/3}-W^{1/3})}{3m^{2/3}+(2W_0^{1/3}-m^{1/3})(2W^{1/3}-m^{1/3})} + 1.1513\log\left(\frac{m^{1/3}+W_0^{1/3}}{m^{1/3}+W^{1/3}}\right)^3\left(\frac{m+W}{W_s}\right)\right\} \tag{4}$$

where $m = W_s - W_0$.

Therefore when the concentration (C) of the solute in the liquid and the corresponding time elapsed (θ) are measured in the range where the mass transfer coefficient (K) and the shape factor of the solid particles (α_w) are held constant, the rate of solution may be calculated. The rate of solution at any time in this range is taken as $[K\alpha_w W^{2/3}(C_s-C)/V]$. In the case where the dissolved amount is so small that the change in surface area (A) is negligible, the surface area of the solid is practically constant (for example Zn-HCl system), and Eq. (1) is integrated into the following form,

$$\log\frac{C_s}{(C_s-C)} = K'\theta \tag{5}$$

where $K' = KA/2.303V$.

When the observed values of $C_s/(C_s-C)$ are plotted againt θ on log-log paper, the results correlate in a straight line. The rate of solution is given as the product of the slope of the straight line and 2.303 (C_s-C).

Further, in the case where the concentration difference (C_s-C) scarcely changes in magnitude (for example the dissolution of a small amount of a highly soluble crystal), the integrated form of Eq. (1) is,

$$\left\{1-(1-x)^{1/3}\right\} = K''\theta \tag{6}$$

where the dissolved fraction is expressed by $x = 1-(W/W_0)$, and $3K'' = K\alpha_w W_0^{-1/3} \times (C_s-C)$.

Plots of $\{1-(1-x)^{1/3}\}$ *versus* θ correlate as a straight line. From the slope of the curve (K''), the rate of solution is given as,

$$K\frac{A}{V}(C_s-C) = \frac{3K''W}{V} \tag{7}$$

(b) R. H. Wilhelm's Methods[2].

With the following expressions,

$$W_d = W_0 - W, \quad X = W_d/W_s, \quad Y = W_0/W_s, \quad \text{and}$$
$$A = \alpha_v n^{1/3} W^{2/3}/\rho_s^{2/3},$$

the following equation may be derived from Eq. (3),

$$Z = \int_0^X \frac{dX}{(Y-X)^{2/3}(1-X)} = \frac{K\alpha_v n^{1/3} W_s^{2/3}}{\rho_s^{2/3} V}\theta = KA_s\theta/V \qquad (8)$$

When the integration is performed, a functional relation between Z and X is obtained, and by representing the relation on a chart taking Y as the parameter, the values of Z may easily be estimated from the observed values of W_d and θ. Hence the rate of solution may be calculated by means of the following relation,

$$K\frac{A}{V}(C_s - C) = \frac{Z}{\theta}\frac{A(C_s-C)}{A_s V} = \frac{Z(W_s - W_0 + W)W_0^{2/3}}{V^2\theta W_s^{2/3}} \qquad (9)$$

(c) Graphical Differentiation Method.

In the case where the change in surface area of the solid particles and the change in concentration in the liquid are rather small, the solution rate curve is almost a straight line, and the rate of solution may easily be obtained from the slope of the tangent line at any point of this curve.

2. 2. Determination of the Mass Transfer Coefficient.

The mass transfer coefficient K may be estimated, when the effective surface area of the solid particles for mass transfer, or a surface shape factor of the solid particle is given [for instance the constant α_w or α_v in Eq. (2) or (6) respectively].

3. Comparison of the Rates of Solution Calculated by Several Methods.

(a) In the Case of Negligible Surface Area Change.

The Zn–HCl system was discussed as such an example in the previous paper[1].

(b) In the Case of Negligible Change in Concentration.

As the solubility of NaCl in water is 282 g NaCl per 785 cc H_2O, the concentration change, *i.e.*, the change in the value of $(C_s - C)$, that occurred when 2.00 g of NaCl was dissolved in 785 cc is negligible. Hence Eq. (6) is applicable. **Fig. 3** is the plot of the observed values of $\{1-(1-x)^{1/3}\}$ *versus* θ for 8~10 mesh spherical NaCl-H_2O system. Experimental conditions are indicated in the lower part of the figure. The initial rate of solution is given by the product of the tangent to the curve and $3W_0/V$ [refer to Eq. (7)]. The plotted points shown

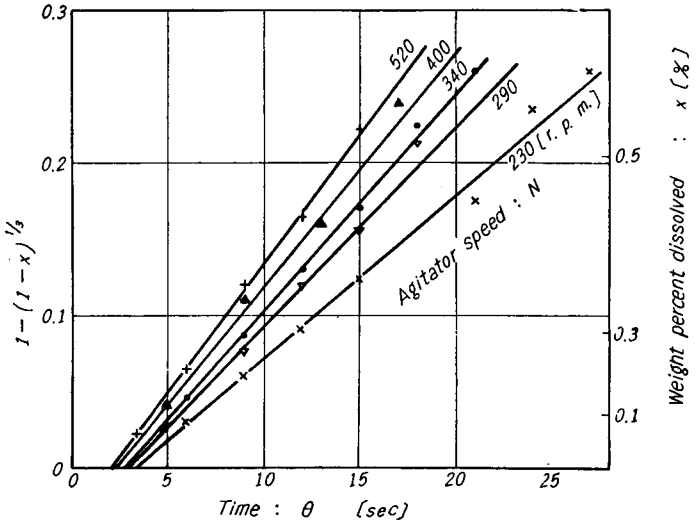

Fig. 3. Plots of $\{1-(1-x)^{1/3}\}$ *vs.* θ for spherical NaCl-H_2O system.
Solid used=2.00 [g] (8~10 mesh).
Temp. =25.0°C.

by the symbol + on curve (1) in **Fig. 4** shows the relation between the rate of solution (R/V) mentioned above and the rotational speed of the impeller (N). Curves (2), (3), (4) and (5) in **Fig. 4** are the plots obtained by the same procedures for the sample of different size.

(c) Comparison of the Results Calculated by Several Methods.

Curve (1) in **Fig. 4** is an example showing the values of the rate of solution $(-dW/Vd\theta)_{\theta=0}$ for 8~10 mesh spherical NaCl calculated by the three methods mentioned above. **Fig. 5** shows the results for the 60~100 mesn $K_2Cr_2O_7$-H_2O system. **Fig. 6**

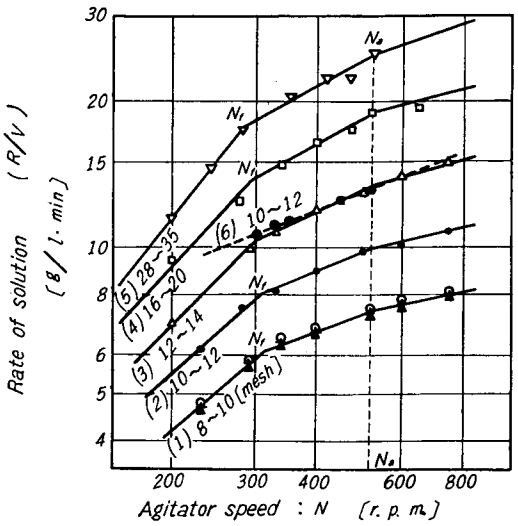

Symbol	Method of calculation for curve (1)
▲	By the Hixson-Crowell's method
+	By Eq. (4)
○	By the Wilhelm's method

Fig. 4. Plots of (R/V) *vs.* N for spherical NaCl-H_2O system.

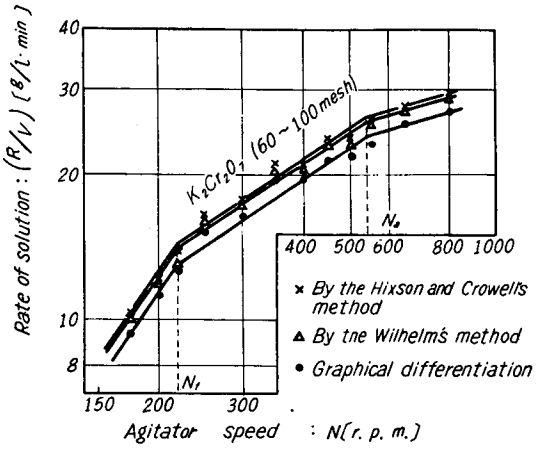

Fig. 5. Comparison of the three methods for estimating the rate of solution (R/V) in the case of the $K_2Cr_2O_7$–H_2O system.
Solid used=2.50 [g/l].
Temp. =25.0°C.

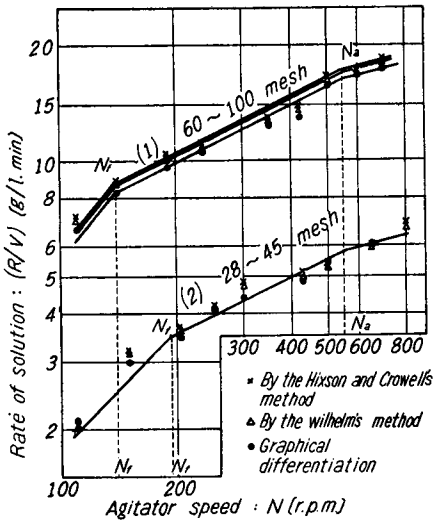

Fig. 6. Comparison of the three methods for estimating the rate of solution (R/V) in the case of the H_3BO_3–H_2O system.
Experimental conditions are the same as those shown in Fig. 5.

shows the results for the spherical H_3BO_3–H_2O system. Curve (1) in this figure is the plot for the small particle size (60~100 mesh) and curve (2) is that for the rather large particle size (28~45 mesh). From these results it may be seen that the values calculated by the three methods are in agreement except in the case of very small particles whose rate of solution is so rapid that experimental errors may be included. Furthermore it should be noted that the slope of these curves (the rate of increase in solution velocity with increase in agitator speed) calculated by the three methods agree well each other.

4. Examination of the Mass Transfer Coefficient.

Since the size and shape of the solid particles change in accordance with the process of solution, the mass transfer coefficient (K) and the shape factor (α_w or α_v) are also expected to change gradually. However, the rate of solution or the rate constant must be determined at the corresponding time elapsed. Hence the authors examined the change in shape factor, mass transfer coefficient and the product of these two. First of all it was ascertained that a spherical particle maintains its spherical shape while it dissolves in the agitated liquid.

It is also seen that the plots of $\{1-(1-x)^{1/3}\}$ *vs.* θ correlate by a straight line until the fraction dissolved amounts to about 30%, in the case of the spherical

$NaCl$–H_2O system as shown in **Fig. 3.** From that result, the mass transfer coefficient for spherical particles may be regarded as constant until the fractional dissolution reaches 30%.

Rearrainging the results for the $K_2Cr_2O_7$–H_2O system shown in **Fig. 5,** the values of Z which are estimated by use of Eq. (8) are plotted against the corresponding time elapsed as shown in **Fig. 7.** In Eq. (8), n, W_s and ρ_s are all fixed values, so that the value Z must be proportional to the time elapsed θ, provided that the product $K\alpha_v$ is held constant. As shown in **Fig. 7,** it is evident that the product $K\alpha_v$ remains almost constant until the weight percent of the dissolved solute reaches a value of at least 25% (refer to the right hand side ordinate). Thus it is concluded that the errors are negligible, when the rate of solution is calculated by the Hixson-Crowell equation or by Wilhelm's method within the range where the fractional dissolution is 25%.

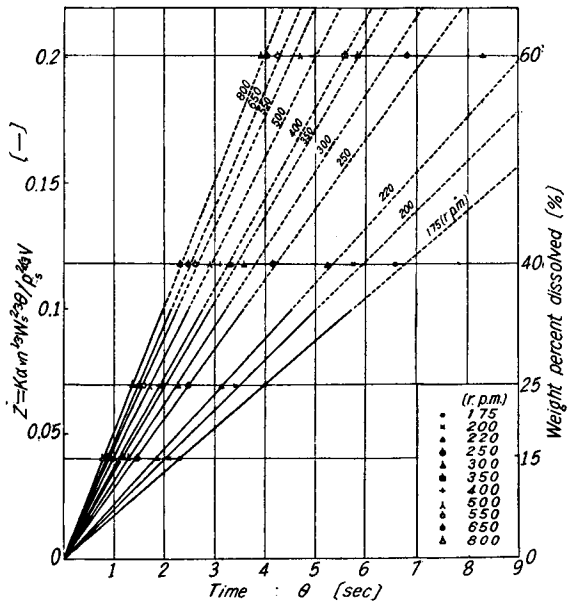

Fig. 7. Diagram showing constancy of the product of the mass transfer coefficient K and the shape factor α_v.

5. Effect of the Increase in Agitator Speed.

Plots of the rate of solution (R/V) *versus* agitator speed are correlated by a straight line on log-log paper. Thus,

$$K \propto N^p \tag{10}$$

Figs. 4, 5 and **6** are examples, where the slope of the curve represents the rate of increase in the dissolution velocity or mass transfer coefficient with the increase in agitator speed. The authors denote this value as "p".

From the experimental results, it is found that the relation between the rate of solution and the agitator speed is represented by a straight line which bends at the agitator speeds of N_f and N_a, where N_f is the critical agitator speed at which the fluidization of all particles occurs and N_a is the critical agitator speed at which the suction of air occurs.

The authors denote the slope of the curve in the range of agitator speed greater than N_f and less than N_a as p_2, and also denote the exponent p as p_1 and p_3 for the ranges of $N \leqq N_f$ and $N_a \leqq N$ respectively by expanding the expression of Eq. (10).

However, as represented by the experimental results shown in **Figs. 4, 5** and **6,** the value of p changes with differences in the type and dimensions of the agitation equipment and with the physical properties such as the viscosity and density of the agitated liquid as well as the size and density of the solid particles. Furthermore it is also disclosed that in a series of geometrically similar agitators the value of p changes with the difference in size factor even though its magnitude is small.

Hence, in order to develop a dimensionless equation representing a general correlation between the variables involved in determining the rate of mass transfer in liquid-solid agitation systems, the correlation between the value of p and related factors is first determined.

5. 1. Effect of the Properties of the Solid Particles.

(a) Experimental Results.

With the agitator speed varying as widely as possible, the amount of solid particles dissolved in pure water and the corresponding time elapsed were measured for various kinds of solid particles (whose density, particle size and shape were widely different, refer to **Table 1**) in the agitator of $D=10$ cm. Form the observed values, the relation between the rate of solution and the agitator speed was obtained by the procedures mentioned above. **Fig.** 8 shows the result for the Zn–HCl system. The relation between the initial rate of solution and the agitator speed are also shown in **Figs. 4, 9, ⋯, 13,** and **14.**

The experimental results show that

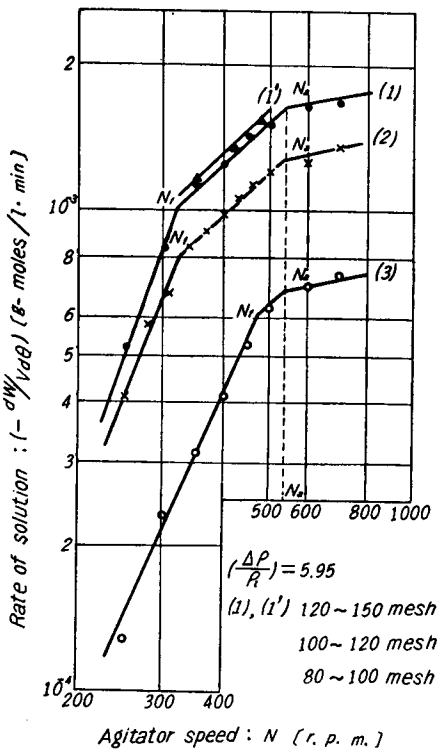

Fig. 8. Correlation of $(-dW/Vd\theta)$ *vs.* N for Zn–HCl system.
Solid particles used=2.50 [g],
HCl =0.00300 [g-moles/*l*],
KNO_3=0.0625 [g-moles/*l*],
Temp. (1), (2) and (3)=10°C,
(1′) =25,0°C.

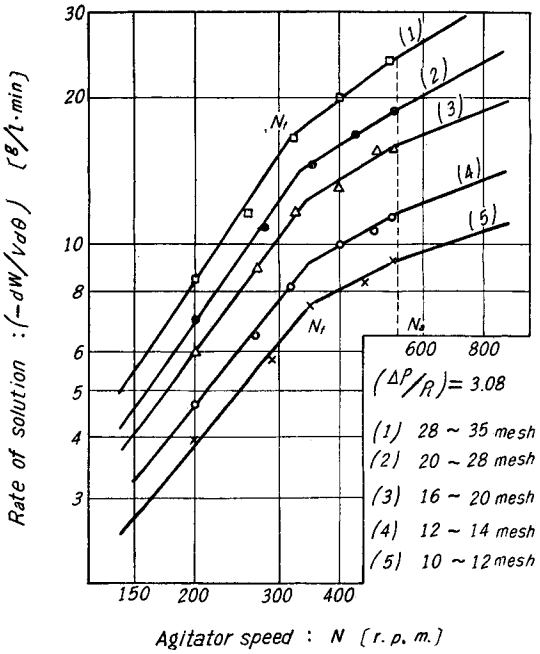

Fig. 9. Plots of $(-dW/Vd\theta)$ *vs.* N for the spherical $AgNO_3$–H_2O system.

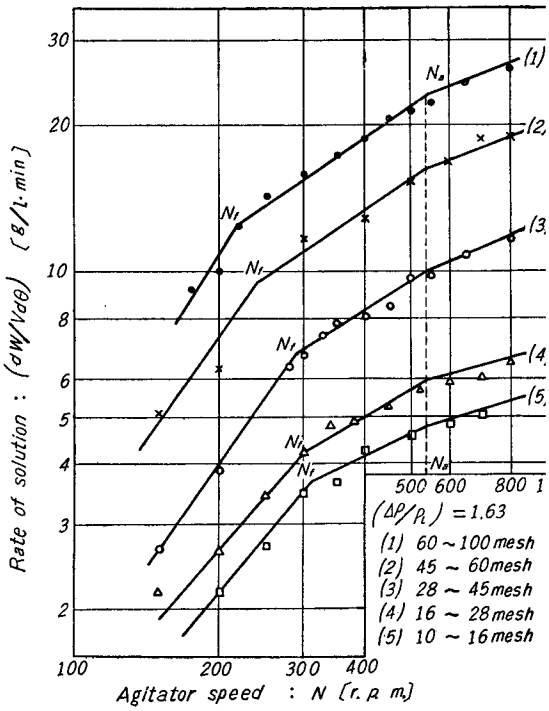

Fig. 10. Correlation of $(-dW/Vd\theta)$ *vs.* N f the $K_2Cr_2O_7$–H_2O system.
Solid particles used=2.00 [g].
Temp.=25.0°C.

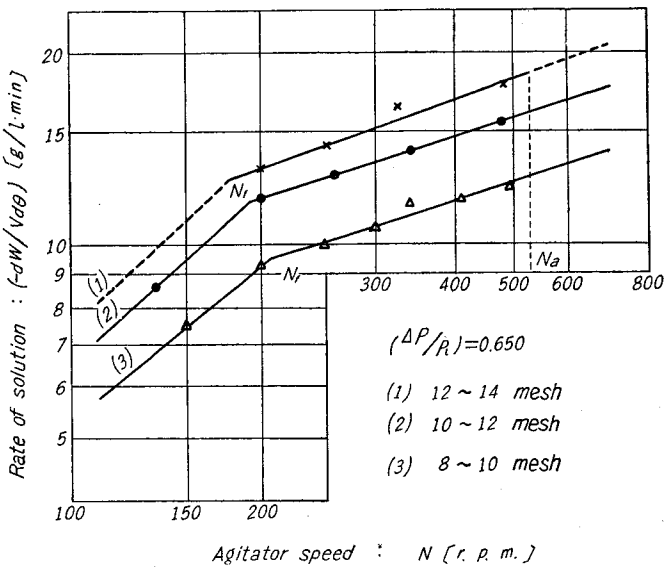

Fig. 11. Plots of $(-dW/Vd\theta)$ *vs.* N for the spherical NH_4NO_3–H_2O system.

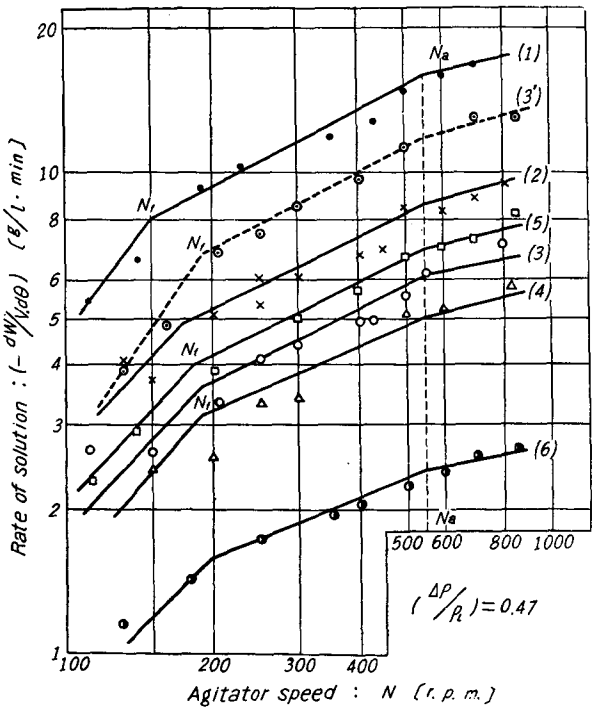

Fig. 12. Correlation of $(-dW/Vd\theta)$ *vs.* N for the H_3BO_3–H_2O system.
Solid used=(1)~(6) 2.00 [g], (3) 4.00 [g], Shape=spherical; size=(1) 60~100 mesh (2) 45~60 mesh (3), (3') 28~45 mesh (d_p=0.519 mm), (4) 16~28 mesh (d_p=0.737 mm)
Shape=triclinic; size=(5) 28~46 mesh (d_p=0.557 mm), (6) 16~28 mesh (d_p=0.858 mm).
Temp.=25.0°C.

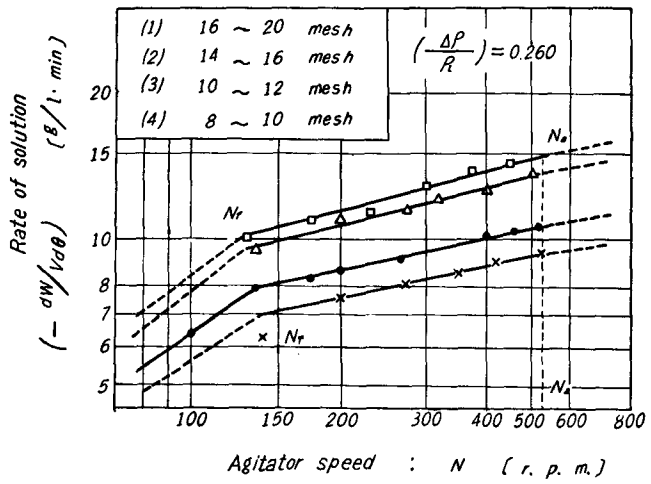

Fig. 13. Plots of $(-dW/Vd\theta)$ *vs.* N for the spherical $CO(NH_2)_2$–H_2O system,

$p_1 > p_2 > p_3$ and these values change with the change in particle size (d_p) and the difference in density between the liquid and solid ($\rho_s - \rho_l$). For example, curve (5) in **Fig. 10** shows the results for rather large particles (10~16 mesh) of $K_2Cr_2O_7$, where p_1 and p_2 are 1.10 and 0.49 respectively, while the values are 1.53 and 0.69 in the case of smaller particles (60~100 mesh). Therefore it may be seen that the smaller the particle size, the larger the value of p. This tendency seems to be true for all samples from zinc powder (sp. gr.=6.95) to crotonic acid (sp. gs.=1.16).

On the other hand, if the value p is compared using samples of different density, it is found that p is larger in the case of solid particles of larger density when the particle size is equal.

Curves (1), (2), (3) and (4) in **Fig. 12** are the results for spherical H_3BO_3 and curves (5) and (6) are those for triclinic crystals. These results show that the slope of the curve p scarcely varies with the difference in the shape of particles, though the absolute values of the rate

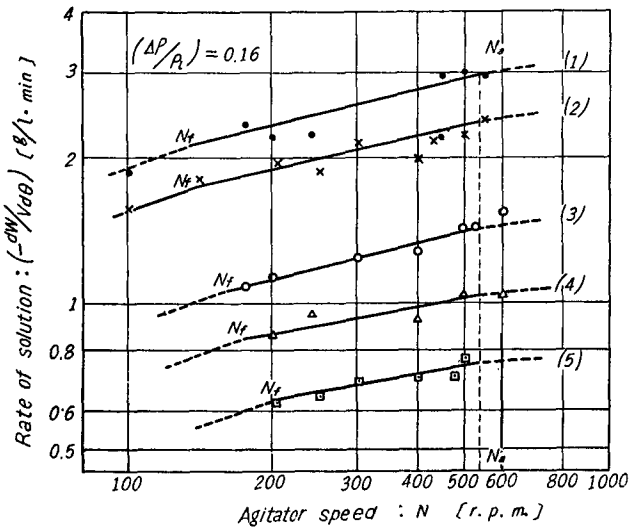

Fig. 14. Correlation of $(-dW/Vd\theta)$ *vs.* N for the crotonic acid-water system.
Solid used=0.500 [g], size=(1) 28~45, (2), (3) 16~28, (4), (5) 10~16 mesh, shape=cubical monoclinic (3), (5), flat monoclinic (1), (2), (4). Temp.=25.0°C.

are different (refer to **Fig. 15**). In addition, curves (1), (2), (3), (4) and (5) in **Fig. 4** are the results for spherical NaCl, and curve (6) is the result for cubic NaCl whose particle diameter d_p is nearly equal to that of curve (2), so that the values of p_2 for both curves are nearly equal.

Curves (3′) and (3) in **Fig. 12** are the plots showing the comparison of the results for the cases where different amounts of solid particles are used. Curve (3) is the plot for 2.00 g of solid and curve (3′) is that for 4.00 g. The rate of solution becomes larger by a factor of 2, but the values of p_2 in both curves are equal. It may be assumed that the flow-pattern of the agitated liquid is hardly affected by the introduction of a small amount of solid particles.

In short, the value of p changes remarkably according to the properties of the solid particles. It is also found that the value changes regularly in proportion to the magnitude of $(\rho_s-\rho_l)$ and d_p. The values of p_1 and p_2 given in **Figs. 4, 8, 9, ⋯, 13** and **14** are measured and tabulated in the last column of **Table 1.**

(b) Determination of the Functional Relation between the Exponent p and the Physical Properties of the Solid.

By means of dimensional analysis the following groups of variables are obtained between the exponent p and the physical properties of the solid, *i.e.*, the difference in density $(\rho_s-\rho_l)$, particle size (d_p) and shape factor of solid particles (ϕ_s).

$$p = F\left\{\left(\frac{\rho_s-\rho_l}{\rho_l}\right), \left(\frac{d_p}{D}\right), \phi_s\right\} \tag{11}$$

The actual functional formula is derived by referring to the experimental results.

For simplicity the value $(\rho_s-\rho_l)/\rho_l$ is denoted as Δ and (d_p/D) as δ, and a

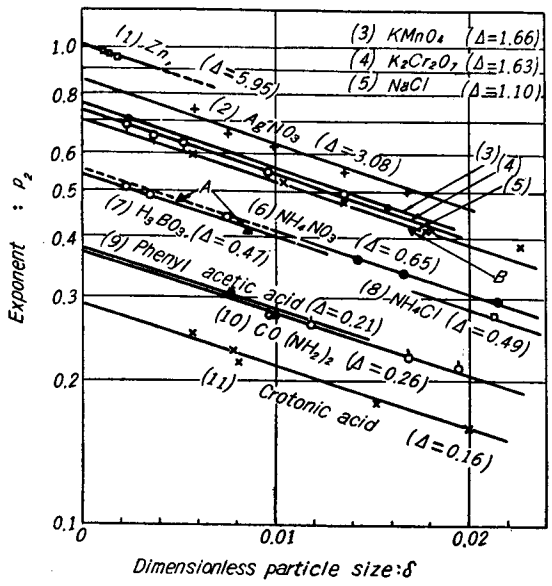

Fig. 15. Correlation of the exponent p_2 *versus* dimensionless particle size δ, where the density difference Δ is taken as the parameter.

symbol $p_{\Delta\delta}$ is used for representing the exponent p which corresponds to the dimensionless ratio of the density difference Δ and the dimensionless ratio of particle size δ.

(1) The Functional Relation between p_2, Δ and δ.

At first, to obtain the relation between p_2 and δ, all the observed values of p_2 are plotted against δ on semi-logarithmic paper taking Δ as the parameter as shown in **Fig. 15.** The relation is nearly linear regardless of the values of Δ. Further, to examine the effect of particle shape upon p_2, the result for triclinic crystals of H_3BO_3 is shown at the two points **A** on curve (7) in **Fig. 15.** The rest of the plotted points on the curve are those for spherical ones. The point **B** on curve (5) is the result for cubic NaCl and the rest are for spherical ones. From these results, the effect of particle shape upon p_2 is found to be insignificant.

Hence, designating the slope of the curve as m, the following relation between $p_{\Delta\delta}$ and δ is given,

$$\log p_{\Delta\delta} = m\delta + \log p_{\Delta 0} \tag{12}$$

Strictly speaking the slope m is slightly different for different values of Δ and shape factor Φ_s. However as these difference are very small, the value $m=-13.5$ is taken from **Fig. 15.** Thus,

$$p_{\Delta\delta} = p_{\Delta 0} \cdot 10^{-13.5\delta} \tag{13}$$

Next, to determine the functional relation between $p_{\Delta\delta}$ and Δ, reading the value of $p_{\Delta\delta}$ at $\delta=0$ in **Fig. 15,** the value $p_{\Delta 0}$ is plotted against Δ as shown on curve (1) in **Fig. 16** where the abscissa is $\Delta+0.043$ (logarithmic scale) and the ordinate is $p_{\Delta\delta}$ (ordinary scale). To make the functional formula valid until Δ is nearly equal to zero, $(\Delta+0.043)$ is taken on the abscissa of the co-ordinate.

From curve (1) in **Fig. 16** the functional relationship between $p_{\Delta 0}$ and Δ is given as,

$$p_{\Delta 0} = 0.48\{\log(\Delta + 0.043) + 1.35\} \tag{14}$$

Combining Eqs. (13) and (14), the dimensionless equation representing the general correlation is obtained as

$$p_{\Delta\delta} \equiv p_2 = 0.48\{\log(\Delta + 0.043) + 1.35\} \cdot 10^{-13.5\delta} \tag{15}$$

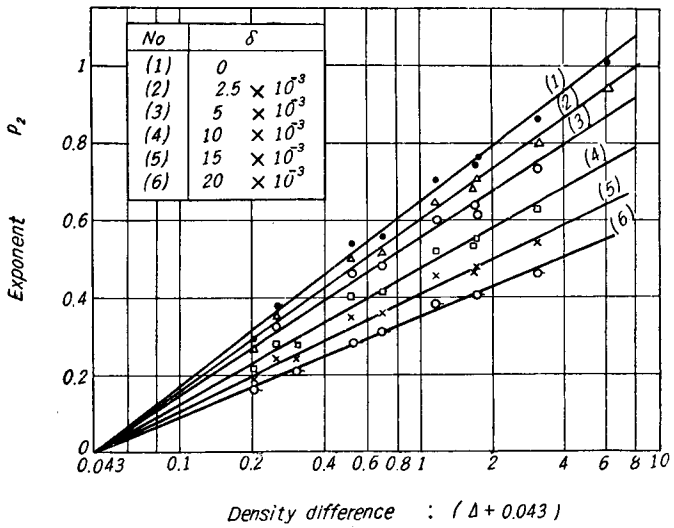

Fig. 16. Relation between the exponent p_2 and the dimensionless density difference $(\Delta+0.043)$, where the dimensionless particle diameter δ is taken as the parameter.

Furthermore curves (2) to (6) in **Fig. 16** are calculated from Eq. (15) and the plotted points are the values obtained by interpolating the observed values shown in **Fig. 15.** Although the absolute value of the rate of solution is not obtainable from the relation shown by Eq. (15), the effect of an increase in agitator speed is indicated.

(2) The Functional Relation between p_1, Δ and δ.

The plots of p_1 *versus* δ where Δ is taken as the parameter are found to be linear on log-log paper (the diagram is omitted). As the slopes of all the straight lines are equal to -0.230, the following relation is obtained,

$$p_1 \delta^{0.230} = \text{constant} \tag{16}$$

Then the values of $p_1\delta^{0.230}$ are calculated from the observed values of p_1 and δ in **Table 1,** and plotted against Δ on log-log paper. The plots are correlated by a straight line (the diagram is omitted) and the following equation is obtained,

$$p_1 = 0.360\Delta^{0.220}\delta^{-0.230} \tag{17}$$

5. 2. Scale Effect upon p (Scale-up of the Apparatus).

Experiments were performed in a series of geometrically similar agitators under condition (1) where the size of the mean particle diameter (d_p) was chosen equal to the similarity ratio of the system, *i.e.*, holding the ratio (d_p/D) constant, and (2) where the same sample (equal d_p) was used in common for all vessels of different diameter. Pure water was used as the agitated liquid and the experiments were conducted with various kinds of solid particles whose density, particle size and shape were different (see **Table 2**).

Fig. 17 is the result for the spherical H_3BO_3–H_2O system whose density difference is rather small ($\Delta=0.470$). All the curves (1), (2), (3) and (4) represent the case where (d_p/D) is taken equal, and the slope of the curves are 0.520, 0.570, 0.615 and 0.660 respectively. There seems to be a tendency for the value of p to become slightly larger with an increase in the vessel diameter D. Curve (1″) is the result for the condition where the particle size is chosen to be 3 times larger than that of curve (1). The slope p_2 of curve (1″) is 0.395 which is smaller than that of curve (1).

Fig. 18 shows the results for the cubic NaCl–H_2O system and is an example of a system where the difference in density between liquid

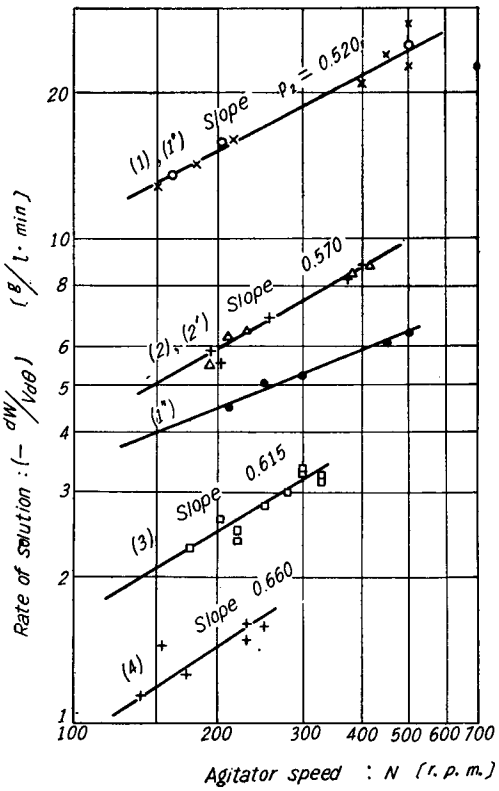

		D	d_p/D	Vessel shape	θ	Solid used
		[cm]	[−]			[g/l]
(1)	×	10	1.95×10^{-3}	flat	90°	3.82
(1′)	○	»	»	dished	»	»
(2)	+	15	»	flat	»	2.55
(2′)	△	»	»	»	45°	»
(3)	□	20	»	»	90°	1.27
(4)	+	30	»	»	»	»
(1″)	●	10	5.85×10^{-3}	»	»	3.82

Fig. 17. Correlation of $(-dW/Vd\theta)$ *vs.* N for the H_3BO_3–H_2O system in geometrically similar systems.
Length of impeller blade: $d=0.5D$;
width of impeller blade: $b=0.1D$;
number of blades: 4;
elevation of impeller: $H_p=0.4D$;
liquid depth: $H_l=D$. Temp.: 25.0°C.

and solid is a little larger. The slope p_2 of curves (1), (2), (3) and (4) for $D=10$, 15, 20 and 30 cm are 0.545, 0.600, 0.640 and 0.710 respectively, revealing the same tendency as for the H_3BO_3–H_2O system, *i.e.*, the value of p becomes larger

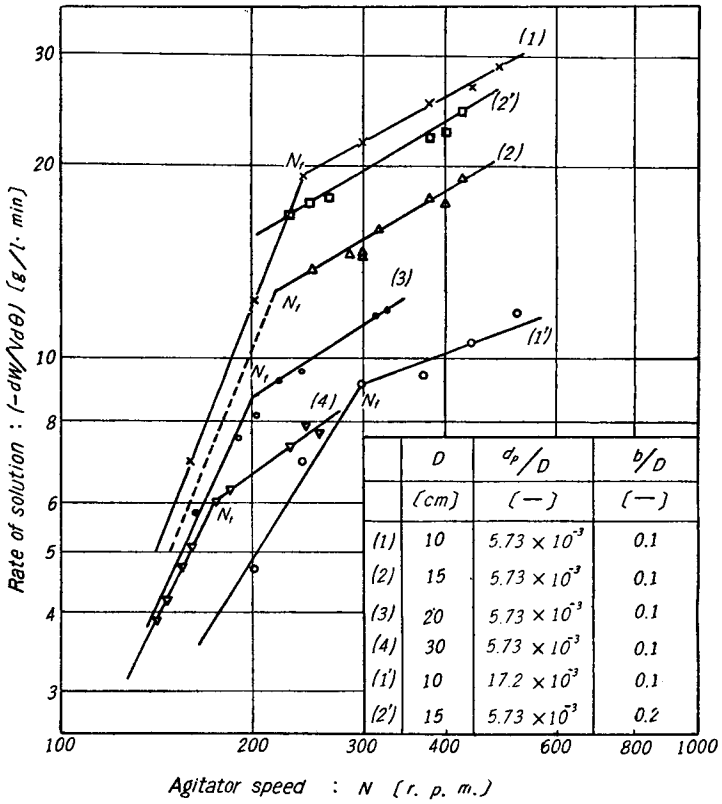

Fig. 18. $(-dW/Vd\theta)$ *vs.* N for NaCl–H_2O system.
Vessel made of plastic with a flat bottom, blade angle: $\theta=90°$C, solid particles used=2.55 [g/*l*]. Temp.=25°C.

with an increase in D. Curve (1′) shows the results for the same system but with a larger size particle and the slope is found to be 0.368, which is smaller than that of curve (1).

Fig. 19 shows the results for the $K_2Cr_2O_7$–H_2O system, where the difference in density is still larger. It is difficult to compare strictly the value of p_2 for $D=30$ cm with the others, because the agitator speed N_f is close to N_a. However, the slope p_2 for curves (1), (2) and (3) are shown to be 0.690, 0.810 and 0.890 respectively. When the particle size is three times as large as that of curve (1), the value of p_2 becomes 0.680 as shown by curve (1″). There is the same tendency as in the case of the H_3BO_3–H_2O and NaCl–H_2O systems, *i.e.*, the

value of p_2 increases with an increase in the size factor of the system (D) in a series of geometrically similar systems [(d_p/D) is fixed], and p_2 decreases with an increase in the particle size (d_p) for the same apparatus [which shows the effect of (d_p/D) in the case where (D) is fixed]. The values of p_2 obtained from the above experimental results [**Figs. 17, 18 and 19**] are plotted against the size factor (D) of the agitation system on semi-logarithmic paper as shown by **Fig. 20.** The plots correlate as straight lines. Curves (1), (2) and (3) are the plots of p_2 *versus* D for the $K_2Cr_2O_7$–H_2O, NaCl–H_2O and H_3BO_3–H_2O systems respectively. Every slope of the curve is nearly equal to 0.230 for different values of Δ $(=\Delta\rho/\rho_l)$ and δ $(=d_p/D)$. Thus the following relation is derived between p_2 and D for a geometrically similar agitation system.

$$p_2 \propto D^{0.230} \qquad (18)$$

As will become more clear in the following paragraph, this result gives a criterion for the scaling up of the agitator.

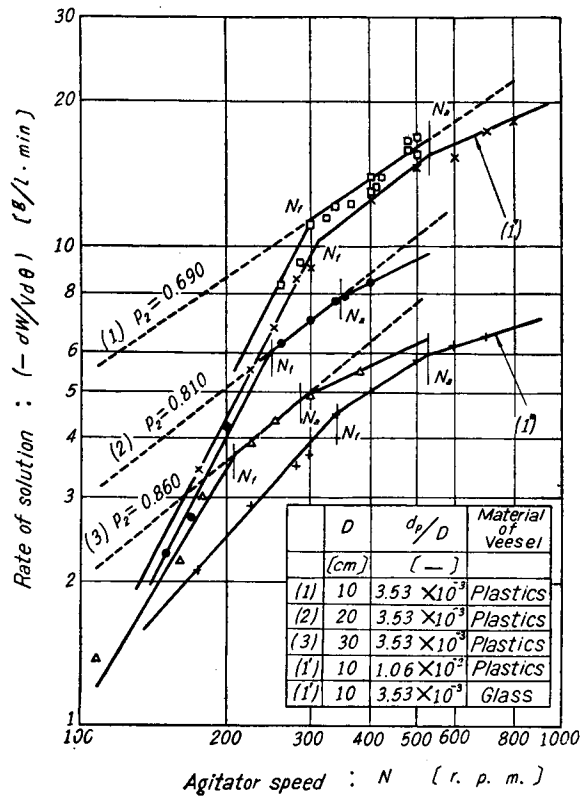

Fig. 19. $(-dW/Vd\theta)$ *vs.* N for $K_2Cr_2O_7$–H_2O system. Width of impeller blade: b=0.1D, blade angle: θ=90°, Solid used=2.55 [g/l]. Temp.=25.0°C.

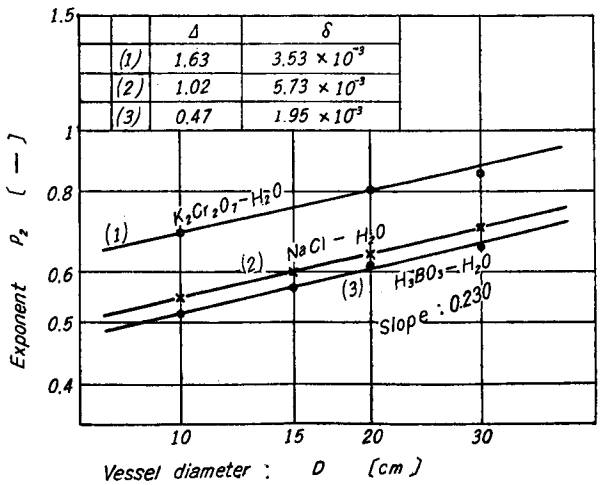

Fig. 20. Correlation of exponent p_2 *vs.* vessel diameter D for geometrically similar systems.

5. 3. Effect of the Viscosity and Density of the Agitated Liquid.

Let the relation between p, μ and ρ_l be determined. For various combinations of solid and liquid whose physical properties are widely different, the authors measured the rate of solution.

As solid materials, $K_2Cr_2O_7$ ($\rho_s=2.63$) of 16~28 and 28~45 mesh, NaCl ($\rho_s=2.02$) of 10~12 and 16~28 mesh, and crotonic acid ($\rho_s=1.16$) of 10~16, 16~28, and 20~28 mesh were used. Aqueous solutions of P.V.A. (1.50, 2.00 and

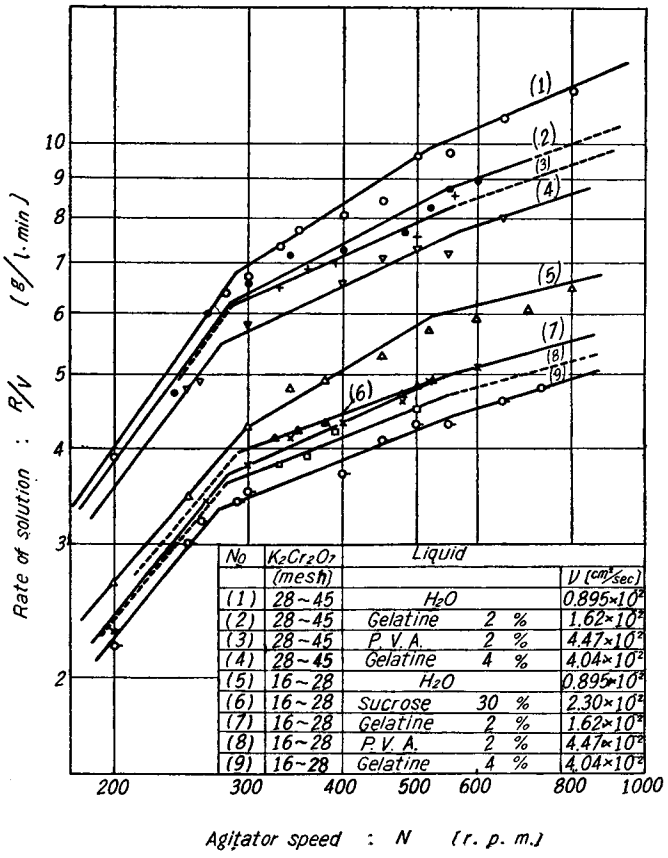

Fig. 21. Plots of (R/V) *vs.* N for systems of $K_2Cr_2O_7$ with liquids of various viscosity.

2.50 percent by weight), gelatine (2.00, 4.00 and 6.00% wt), sucrose (15.0 and 30.0% wt) and glycerine (25%) were used (refer to **Table 3**). The relation between the observed values of the rate of solution and the agitator speed for the systems mentioned above are shown in **Figs. 21, 22** and **23.** In all systems, it is found that both the absolute value of the rate of solution and the slope of the curve p_2 decrease with an increase in the viscosity of the agitated liquid.

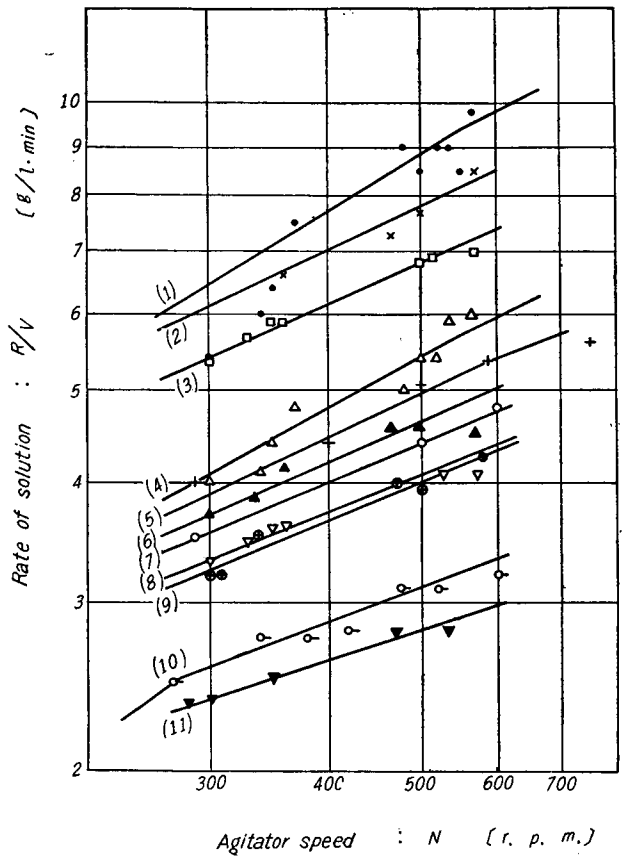

No.	Symbol	Solid	Liquid		
		[mesh]			ν [cm²/sec]
1	—●—	16~28	H_2O		0.895×10^{-2}
2	—×—	»	P.V.A.	1.5%	2.90 »
3	—□—	»	P.V.A.	2.5%	5.50 »
4	—△—	10~12	H_2O		0.895 »
5	—+—	»	Gelatine	2 %	1.62 »
6	—▲—	»	P.V.A.	1.5%	2.90 »
7	—○—	»	Gelatine	4 %	4.04 »
8	—▽—	»	P.V.A.	2.5%	5.50 »
9	—⊕—	»	Sucrose	5 %	1.29 »
10	—○--	»	Glycerine	25 %	1.68 »
11	—▼--	»	Sucrose	30 %	2.30 »

Fig. 22. Plots of (R/V) *vs.* N for systems of NaCl with liquids of various viscosity.

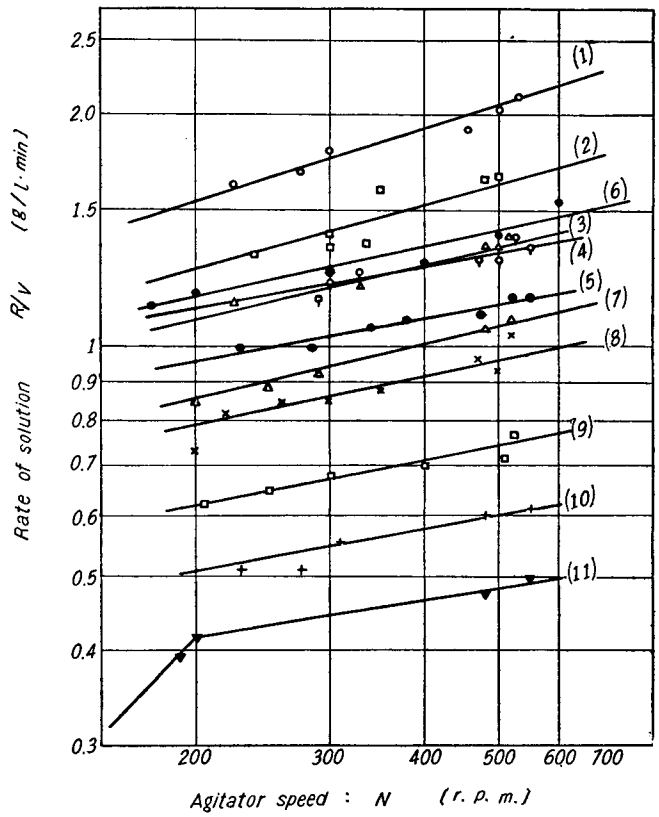

No.	Symbol	Soid	Liquid		
		[mesh]			ν [cm²/sec]
4	—○—	20~28	H_2O		0.895×10^{-2}
1	—□—	〃	P.V.A.	1.5%	2.90 〃
2	—△—	〃	P.V.A.	2.5%	5.50 〃
3	—○—	〃	Sucrose	15 %	1.29 〃
5	—⊕—	〃	Glycerine	25 %	1.68 〃
6	—●—	16~28	H_2O		0.895 〃
7	—▲—	〃	Gelatine	4 %	4.04 〃
8	—×—	〃	Gelatine	6 %	5.59 〃
9	—■—	10~16	H_2O		0.895 〃
10	—+—	〃	Gelatine	2 %	1.62 〃
11	—▼—	〃	Gelatine	4 %	4.04 〃

Fig. 23. Plots of (R/V) *vs.* N for systems of crotonic acid with liquids of various viscosity.

For example, in **Fig. 22,** curve (4) is the result for H_2O (μ=0.885 c.p.)-NaCl of 10~12 mesh, while curves (5), (6), (7) and (8) are the results for the aqueous solutions of gelatine 2% (μ=1.62), P.V.A. 1.5% (μ=2.90), gelatine 4% (μ=4.04) and P.V.A. 2.5% (μ=5.50) respectively for the same solid particles, *i.e.*, the results for systems where only the viscosity of the liquid is increased, the density being nearly equal to 1.00 g/cm³. Similarly, curves (9), (10) and (11) show the results

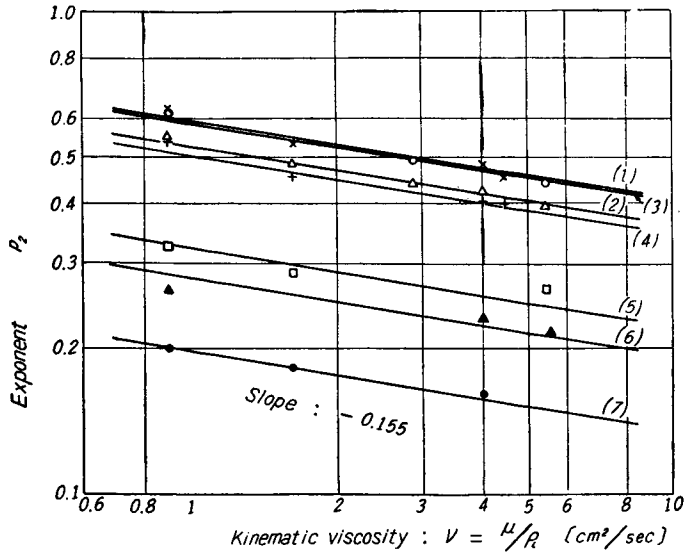

No.	Symbol	Solid		Impeller blade	
			[mesh]	b [cm]	θ
1	○	NaCl	16~28	1.00	45°
2	△	"	10~12	"	"
3	×	$K_2Cr_2O_7$	28~45	1.50	75°
4	+	"	16~28	"	"
5	□	Crotonic acid	20~28	"	"
6	▲	"	16~28	"	"
7	●	"	10~16	"	"

Fig. 24. Plots of exponent p_2 *vs.* ν.

for aqueous solutions of 15% sucrose (ρ_l=1.06, μ=1.29 c.p.), 25% glycerine (ρ_l=1.06, μ=1.68), and 30% sucrose (ρ_l=1.13, μ=2.30) respectively for the H_2O–NaCl system where both the density and the viscosity change.

As the effect of both the decrease in the difference in density and the increase in viscosity reinforce each other, the decrease in both the rate of solution and the slope p are found to be remarkable.

From these experimental results, the values of the slope p_2 for various systems [**Figs. 21, 22** and **23**], where the liquid density is nearly equal to 1.00 [g/cm^3] and the viscosity is different, are plotted against the liquid viscosity (ν) on log-log paper as shown in **Fig. 24.** The relation between p_2 and ν is approximated by a linear relation. Though the absolute value of the slope p_2 is of course different with the change in density and size of the solid particles, the rate of decrease of the slope p_2 caused by the increase in viscosity (the slope of the curves in **Fig. 24**) is equal to -0.155 regardless of the properties of the solid particles. Hence the following relation is obtained.

$$p_2 \propto \nu^{-0.155} \tag{19}$$

Although Eq. (11) was already presented as the functional relation between the slope p_2 and the physical properties of the solid, it was found that the effects of dimension (D), the acceleration due to gravity (g) and the liquid viscosity (ν) upon p must not be neglected, so that the following groups of variables are given by dimensional analysis.

$$p = F'\left\{\left(\frac{\rho_s-\rho_l}{\rho_l}\right), \left(\frac{d_p}{D}\right), \left(\frac{D^3g}{\nu^2}\right), \Phi_s\right\} \tag{20}$$

Eq. (15) was already obtained for the various systems where the values of ρ_s, d_p and Φ_s were different, and D, g and ν were equal. The relation between p and D was represented by Eq. (18) for various systems having equal values of $(\rho_s-\rho_l)/\rho_l$, (d_p/D), (ν) and (Φ_s). In addition, Eq. (19) was also determined for various systems, where the physical properties of the solid particles were different and the viscosity of liquid was changed but holding the values of $(\rho_s-\rho_l)/\rho_l$, (d_p/D), (Φ_s) and (D) constant. These two equations are rewritten in the following form,

$$p_2 \propto (D^3)^{0.0767} \tag{21}$$

$$p_2 \propto (1/\nu^2)^{0.0775} \tag{22}$$

Taking the mean values of the exponent of Eqs. (21) and (22), we have,

$$p_2 \propto \left(\frac{D^3g}{\nu^2}\right)^{0.0772} \tag{23}$$

Hence the following dimensionless equation is derived combining the results of Eqs. (15) and (23) which represents the correlation of the variables involved (p_2, ρ_s, d_p, Φ_s, ρ_l, ν, D and g).

$$p_2 = 0.0802\left(\frac{D^3g}{\nu^2}\right)^{0.0772}\left\{\log(\Delta+0.043)+1.35\right\}\cdot 10^{-13.5\delta} \tag{24}$$

The values of p_2 calculated by Eq. (24) are shown by curve (6) in **Fig. 21,** curves (9), (10) and (11) in **Fig. 22** and curves (4) and (5) in **Fig. 23.**

The plots of the experimental results agree quite well with the calculated line. Thus it is proved that Eq. (24) is valid for systems where both the density and the viscosity of the liquid vary.

6. The Agitator Speed at which Fluidization of the Solid Particles (N_f) and Aeration Occur (N_a).

As long as the amount of solid particles used is not large, the agitator speed (N_a) at which aeration occurs is observed to be the same regardless of the physical properties of the solid.

The relation between N_a and D for a geometrically similar agitation system is shown by curve (1) in **Fig. 25.** Curve (2) is the result where a 3% aqueous solution of P.V.A. (ρ_l=1.07, μ=9.79 c.p.) is used.

Hence the following relation is obtained between N_a and D.

$$N_a \propto D^{-2/3} \qquad (25)$$

One of the authors[5] obtained the following experimental equation representing the agitator speed at which fluidization of the solid particles occurred.

$$N_f = KD^{-2/3} d_p^{1/3} \left(\frac{\rho_s - \rho_l}{\rho_l}\right)^{2/3} \times \left(\frac{\mu}{\rho_l}\right)^{1/9} \left(\frac{V_p'}{V_p}\right)^{-0.7} \qquad (26)$$

Hence under the conditions of the same values of ρ_s, ρ_l, μ and shape factors, Eq. (26) may be rewritten as follows,

$$N_f \propto (d_p/D)^{1/3} D^{-1/3} \qquad (27)$$

Therefore when the value (d_p/D) is constant, it is expected that the value

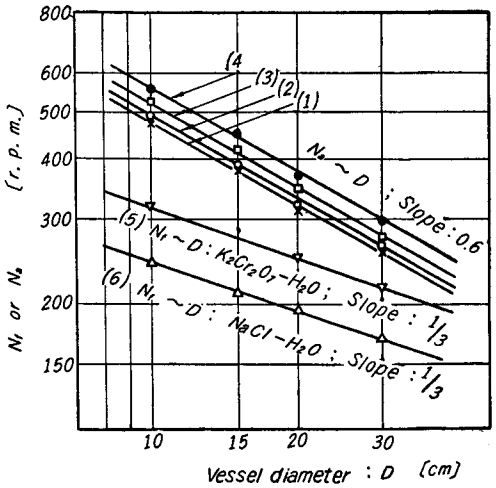

No.	Symbol	Agitated liquid	Impeller blade angle	Elevation of impeller
			θ	H_p
(1)	×	H_2O	90°	4
(2)	○	P.V.A. 3% aq. soln	"	"
(3)	□	H_2O	45°	"
(4)	●	"	90°	2
(5)	▽	"	"	4
(6)	△	"	"	"

Fig. 25. Plots of the agitator speed N_a (suction of air) and N_f (fluidization of particles) *vs.* vessel diameter D for geometrically similar systems.
Vessel with a flat bottom, length of impeller blade: d=0.5 D; width of impeller blade: b=0.1 D; number of blades: 4; liquid depth: H_l=D. Temp.: 25.0°C.

N_f will be proportional to $D^{-1/3}$. [Strictly speaking, it seems more reasonable to take into account the effect of the Froude number as shown by Eq. (24)].

The values of N_f for the NaCl–H_2O and $K_2Cr_2O_7$–H_2O systems shown in **Figs. 18** and **19** are plotted against D on log-log paper, from which curves (5) and (6) in **Fig. 25** are obtained. The relation represented by Eq. (27) is satisfied fairly well in both systems.

7. A General Correlation for Mass Transfer in Agitated Liquid-Solid Systems.

7.1. Development of a General Form of Dimensionless Equation.

When the thickness of the effective diffusional film (x) is defined as the ratio of the diffusion coefficient (D_f) to the mass transfer coefficient (K) [refer to Eq. (1) in the previous paper[1]], the variables affecting the value of x may be taken as follows in a series of geometrically similar agitators: the characteristic length of the system (*i.e.*, size factor d_p or D), the relative velocity between liquie and solid (u), the liquid density (ρ_l), the liquid viscosity (μ), the density of solid (ρ_s) and the acceleration due to gravity (g).

Provided the Rynolds number (Re), Froude number (Fr) and dimensionless density difference ($\Delta\rho/\rho_l$) are equal in geometrically similar agitation systems, these systems are also dynamically similar. Hence it seems reasonable to adopt a dimensionless equation involving the groups mentioned above to correlate x and other variables. Thus the following equation is derived.

$$\left(\frac{d_p}{x}\right) = C'\left(\frac{d_p u}{\nu}\right)^{\alpha}\left(\frac{u^2}{d_p g}\right)^{\beta}\left(\frac{\Delta\rho}{\rho_l}\right)^{\gamma} \tag{28}$$

or

$$\left(\frac{D}{x}\right) = C'\left(\frac{Du}{\nu}\right)^{\alpha}\left(\frac{u^2}{Dg}\right)^{\beta}\left(\frac{\Delta\rho}{\rho_l}\right)^{\gamma} \tag{29}$$

In practical agitation problems, various solid particles whose ρ_s, d_p and ϕ_s are different will be handled.

Hence, by including these factors, the following relation is obtained,

$$\left(\frac{D}{x}\right) = C''\left(\frac{Du}{\nu}\right)^{\alpha}\left(\frac{u^2}{Dg}\right)^{\beta}\left(\frac{\Delta\rho}{\rho_l}\right)^{\gamma}\left(\frac{d_p}{D}\right)^{\delta}(\phi_s)^{\varepsilon} \tag{30}$$

or

$$\left(\frac{D}{x}\right) = C''\left(\frac{Du}{\nu}\right)^{\alpha''}\left(\frac{\nu^2}{D^3 g}\right)^{\beta}\left(\frac{\Delta\rho}{\rho_l}\right)^{\gamma}\left(\frac{d_p}{D}\right)^{\delta}(\phi_s)^{\varepsilon} \tag{31}$$

where $\alpha''=\alpha+2\beta$.

In general, the relation is rewritten as follows.

$$\left(\frac{D}{x}\right) = F_0\left\{\left(\frac{Du}{\nu}\right), \left(\frac{\nu^2}{D^3 g}\right), \left(\frac{\Delta\rho}{\rho_l}\right), \left(\frac{d_p}{D}\right), \phi_s\right\} \tag{32}$$

The particular functional relation among the dimensionless groups is determined by referring to the experimental results.

As the variables relating the mass transfer coefficient K are proved to be x, D_f, ν and D from the experimental results shown in **Figs. 4, 8, ⋯, 13** and **14,** the following relation is obtained by dimensional analysis.

$$\left(\frac{KD}{D_f}\right) = C'''\left(\frac{D}{x}\right)^{\lambda}\left(\frac{\nu}{D_f}\right)^{\omega} \tag{33}$$

Combination of Eqs. (31) and (33) results in,

$$\left(\frac{KD}{D_f}\right) = C\left(\frac{Du}{\nu}\right)^{\alpha'}\left(\frac{\nu}{D_f}\right)^{\beta'}\left(\frac{\nu^2}{D^3g}\right)^{\gamma'}\left(\frac{\Delta\rho}{\rho_l}\right)^{\delta'}\left(\frac{d_p}{D}\right)^{\varepsilon'}(\Phi_s)^{\lambda'} \tag{34}$$

or

$$\left(\frac{KD}{D_f}\right) = C\left(\frac{Du}{\nu}\right)^{\alpha'}\left(\frac{\nu}{D_f}\right)^{\beta''}\left(\frac{D_f^2}{D^3g}\right)^{\gamma'}\left(\frac{\Delta\rho}{\rho_l}\right)^{\delta'}\left(\frac{d_p}{D}\right)^{\varepsilon'}(\Phi_s)^{\lambda'} \tag{35}$$

where $\beta''=\beta'+2\gamma'$.

In a general form, the relation is expressed by,

$$\left(\frac{KD}{D_f}\right) = F_1\left\{\left(\frac{Du}{\nu}\right), \left(\frac{\nu}{D_f}\right), \left(\frac{D_f^2}{D^3g}\right), \left(\frac{\Delta\rho}{\rho_l}\right), \left(\frac{d_p}{D}\right), \Phi_s\right\} \tag{36}$$

where u is the relative velocity between the solid particle and the liquid-bulk. As it is advantageous to use the rotational speed of the impeller (n) instead of the relative velocity (u), the authors derived a relation between u and n involving other variables. The factors affecting the relative velocity u are d_p, ρ_s, Φ_s, ρ_l, ν, g, D and n, so that the following equation is obtained.

$$\left(\frac{Du}{\nu}\right) = f\left\{\left(\frac{D^2n}{\nu}\right), \left(\frac{\nu^2}{D^3g}\right), \left(\frac{\Delta\rho}{\rho_l}\right), \left(\frac{d_p}{D}\right), \Phi_s\right\} \tag{37}$$

By combining the Eqs. (36) and (37), we also have the final form,

$$\left(\frac{KD}{D_f}\right) = F_2\left\{\left(\frac{D^2n}{\nu}\right), \left(\frac{\nu}{D_f}\right), \left(\frac{D_f^2}{D^3g}\right), \left(\frac{\Delta\rho}{\rho_l}\right), \left(\frac{d_p}{D}\right), \Phi_s\right\} \tag{38}$$

Eq. (38) is the fundamental equation for the general correlation, and the functional relation is determined by referring to the experimental results as mentioned later.

7. 2. Determination of the Dimensionless Equation of General Form.

(a) Relation between the Mass Transfer Coefficient and the Agitator Speed.

The relation expressed by Eq. (10) is confirmed by the experimental results shown in **Figs. 2, 3, ⋯, 7** and **8.** Hence for the systems where ρ_s, ρ_l, d_p, D, Φ_s, D_f, ν and g are all fixed, we have,

$$\left(\frac{KD}{D_f}\right) \propto \left(\frac{D^2n}{\nu}\right)^{p} \tag{39}$$

where the exponent p is given by Eq. (24).

(b) Relation between the Mass Transfer Coefficient and the Size Factor in a Geometrically Similar System.

The experimental results shown in **Figs. 17, 18** and **19** represent a comparison of the rate of solution of solid particles in a series of geometrically similar agitators. In those experiments the ratio of the particle size d_p is equal to the similarity ratio of the agitators. For any particular liquid-solid combination [*i.e.*, (ν/D_f) and $(\Delta\rho/\rho_l)$ are fixed] under geometrically similar conditions [*i.e.*, (d_p/D) and (ϕ_s) are fixed] Eq. (36) is rewritten as,

$$\left(\frac{KD}{D_f}\right) = \left(\frac{D^2n}{\nu}\right)^p f_1\left(\frac{D_f^2}{D^3g}\right) \tag{39'}$$

Further the effective surface area of the solid particles for mass transfer (A) in Eq. (3) is expressed by the following definition using a surface shape factor: $\phi \equiv A/nd_p^2$,

$$A = \phi_s n d_p^2 = \left(\frac{\phi_s}{\pi}\right) n\pi d_p^2 \tag{40}$$

When the value of ϕ_s is given, the value of A is easily estimated. However in many cases the correct value of ϕ_s is practically unknown. Therefore the authors made the following substitution,

$$K\left(\frac{\phi_s}{\pi}\right) \equiv K' \tag{41}$$

Then K' is easily estimated by the relation,

$$K' = \left(-\frac{dW}{Vd\theta}\right) \Big/ \frac{n\pi d_n^2}{V}(C_s - C) \tag{42}$$

As K' is a value proportional to K in the range where the shape factor of solid particles (ϕ_s) is unchanged, Eq. (39) may be rewritten,

$$\left(\frac{K'D}{D_f}\right) = \left(\frac{D^2n}{\nu}\right)^p f_1\left(\frac{D_f^2}{D^3g}\right) \tag{43}$$

or

$$\left(\frac{K'D}{D_f}\right) \Big/ \left(\frac{D^2n}{\nu}\right)^p = f_1\left(\frac{D_f^2}{D^3g}\right) \tag{44}$$

The values $(K'D/D_f)/(D^2n/\nu)^p$ and (D_f^2/D^3g) are calculated from the experimental results shown by curves (1), (2), (3) and (4) in **Fig. 17,** curves (1), (2), (3) and (4) in **Fig. 18** and curves (1), (2) and (3) in **Fig. 19.**

Then $(K'D/D_f)/(D^2n/\nu)^p$ is plotted against (D_f^2/D^3g) on log-log paper as shown by **Fig. 26.**

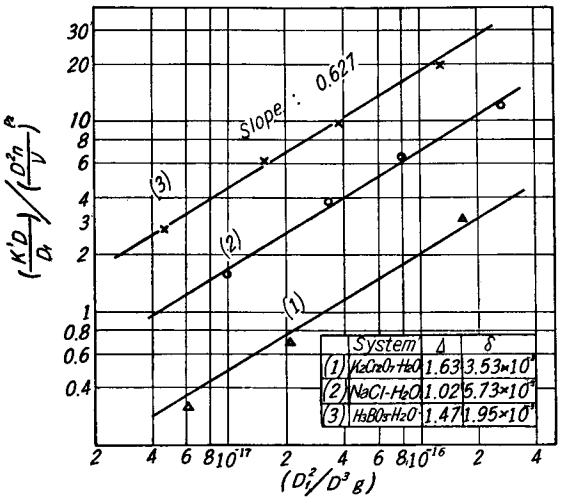

Fig. 26. Correlation of $(K'D/D_f)/(D^2n/\nu)^{p_2}$ *vs.* (D_f^2/D^3g) for geometrically similar systems.

The plots are correlated by a straight line whose slope is 0.627 regardless of the values of $(\Delta\rho/\rho_l)$, (d_p/D) and (Φ_s).

In the case where the same solid and liquid are used, the diffusion coefficient, the density of the solid, the viscosity and density of the liquid are equal, so that in geometrically similar agitation systems, the general form of the dimension-less equation [Eq. (36)] becomes,

$$\left(\frac{KD}{D_f}\right) = C_1\left(\frac{D^2n}{\nu}\right)^{p_2}\left(\frac{D_f^2}{D^3g}\right)^{0.627} \quad (45)$$

(c) Relation between the Mass Transfer Coefficient and the Viscosity of the Agitated Liquid.

The rate of solution of solid particles whose size and density were different was observed in liquids of varying viscosity. The results are shown in **Figs. 21, 22** and **23.** For all of these systems, the values:

$$(K'D/D_f)/(D^2n/\nu)^p(D_f^2/D^3g)^{0.627} \quad \text{and} \quad (\nu/D_f)$$

are calculated, where the values d_p, D, ν, D_f and W are given by the experimental conditions, and the value K' is calculated from the rate data $(-dW/Vd\theta)$ for any agitator speed of n $(=1/60\ N)$ between N_f and N_a. The value p can be estimated by Eq. (24). However, the authors adopted the direct experimental results. A logarithmic plot of $(K'D/D_f)/(D^2n/\nu)^p(D_f^2/D^3g)^{0.627}$ *versus* (ν/D_f) is shown in **Fig. 27.** Though the plots for each solid sample are correlated by a straight line, the slopes are different for different solids.

Reading the slope q in the diagram, the values are plotted against δ $(=d_p/D)$ as shown in **Fig. 28.** The relation between q and δ is approximated by a straight line whose slope is -14.4 for every system.

The intersections on the ordinate axis, *i.e.*, q_0 are 1.94, 1.87 and 1.47 for $K_2Cr_2O_7$–H_2O $(\Delta=1.63)$, NaCl–H_2O $(\Delta=1.22)$ and crotonic acid—H_2O systems $(\Delta=0.16)$ respectively. As a log-log plot of the value q_0 against Δ yields a straight line whose slope is 0.116 as shown in **Fig. 29,** the result is presented in the form:

$$q = -14.4\,\delta + 1.84\,\Delta^{0.116} \quad (46)$$

Hence for a system with the same values of $(\Delta\rho/\rho_l)$, (d_p/D) and Φ_s, the relationship between the variables affecting mass transfer in the liquid-solid agitation systems is,

$$\left(\frac{K'D}{D_f}\right)\Big/\left(\frac{D^2n}{\nu}\right)^p\left(\frac{D_f^2}{D^3g}\right)^{0.627}\propto\left(\frac{\nu}{D_f}\right)^q \tag{47}$$

where the exponent q is given by Eq. (46).

(d) Relation between the Mass Transfer Coefficient and Particle Size.

Figs. 4, 9, 11, 12 and **13** are diagrams showing the rate of solution of spherical crystals of NaCl, $AgNO_3$,

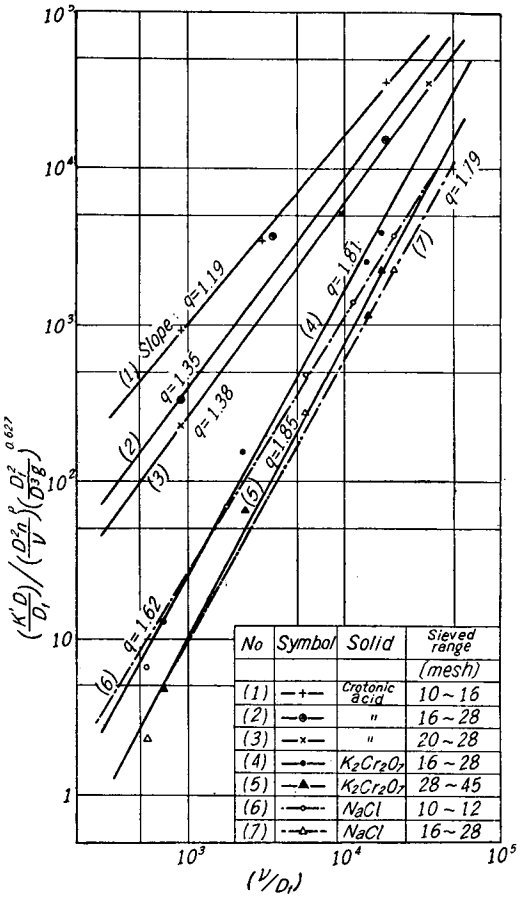

Fig. 27. Correlation of $(K'D/D_f)\times(D^2n/\nu)^p(D_f^2/D^3g)^{0.627}$ *vs.* (ν/D_f).

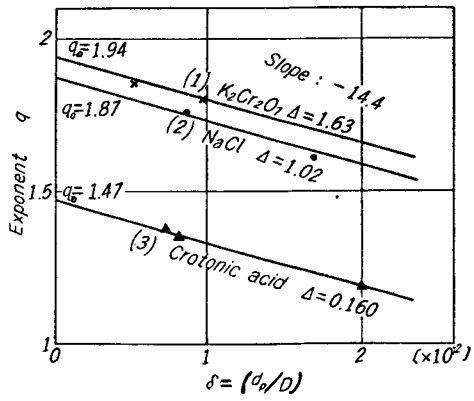

Fig. 28. Plots of q *vs.* δ.

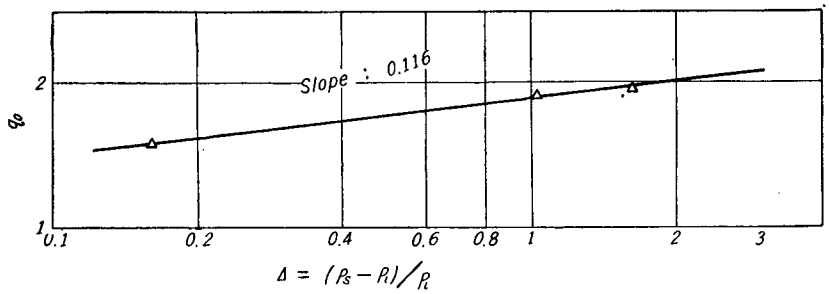

Fig. 29. Plots of q_0 *vs.* Δ.

NH_4NO_3, H_3BO_3 and $CO(NH_2)_2$. From these results, the values

$$(KD/D_f)/(D^2n/\nu)^p(\nu/D_f)^q(D_f^2/D^3g)^{0.627} \quad \text{and} \quad (d_p/D)^2$$

are calculated and plotted on log-log paper as shown in **Fig. 30.** The plots for every system are correlated by a straight line whose slope is 1.54. Hence for the system having the same values of $(\Delta\rho/\rho_l)$ and (ϕ_s), we have,

$$\left(\frac{KD}{D_f}\right)/\left(\frac{D^2n}{\nu}\right)^p\left(\frac{\nu}{D_f}\right)^q\left(\frac{D_f^2}{D^3g}\right)^{0.627} \propto \left(\frac{d_p}{D}\right)^{3.08} \tag{48}$$

(e) Relation between Mass Transfer and the Difference in Density between Liquid and Solid.

From the observed values of the rate of solution of spherical crystals shown in **Figs. 4, 9, 11, 12** and **13,** the values,

$$\left(\frac{KD}{D_f}\right)/\left(\frac{D^2n}{\nu}\right)^p\left(\frac{\nu}{D_f}\right)^q\left(\frac{D_f^2}{D^3g}\right)^{0.627}\left(\frac{d_p}{D}\right)^{3.08}$$

and $\Delta^2 = \left\{(\rho_s-\rho_l)/\rho_l\right\}^2$

are calculated and plotted on log-log paper as shown by the Points **4, 1, 9, 11** and **12** in **Fig. 31.** In addition, for systems with different physical properties of the solid, whose shape is not spherical, and of the liquid, the dimensionless values:

$$\left(\frac{K'D}{D_f}\right)/\left(\frac{D^2n}{\nu}\right)^p\left(\frac{\nu}{D_f}\right)^q\left(\frac{D_f^2}{D^3g}\right)^{0.627}\left(\frac{d_p}{D}\right)^{3.08}$$

and Δ^2

are calculated and plotted in the same figure (**Fig. 31**).

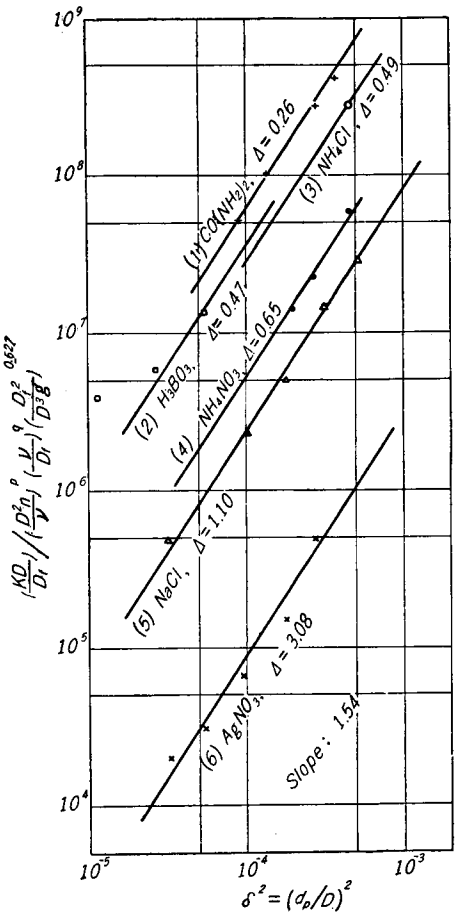

Fig. 30. Correlation of $(Sh)/(Re)^p \times (Sc)^q(D_f^2/D^3g)^{0.627}$ *vs.* δ^2.

Except for the results with solid particles of shapes extremely different from a sphere such as thin leaflets or needles, these plots are correlated by a straight line for the following range of conditions covered by the experiments: $\rho_s=1.16 \sim 6.95$ g/cm^3, $d_p=8 \sim 50$ mesh, $\nu=0.895 \sim 5.59$ c.p. and $D=10 \sim 30$ cm. Hence,

$$\left(\frac{K'D}{D_f}\right)\Big/\left(\frac{D^2n}{\nu}\right)^p\left(\frac{\nu}{D_f}\right)^q\left(\frac{D_f^2}{D^3g}\right)^{0.627}\left(\frac{d_p}{D}\right)^{3.08} \propto \left\{\left(\frac{\rho_s-\rho_l}{\rho_l}\right)^2\right\}^{-1.41} \tag{49}$$

Thus from **Fig. 25** the coeffiient and the exponent of the dimensionless equation of general correlation are determined, as follows,

$$\left(\frac{K'D}{D_f}\right) = 3.60\times10^{12}\left(\frac{D^2n}{\nu}\right)^p\left(\frac{\nu}{D_f}\right)^q\left(\frac{D_f^2}{D^3g}\right)^{0.627}\left(\frac{d_p}{D}\right)^{3.08}\left(\frac{\rho_s-\rho_l}{\rho_l}\right)^{-2.82} \tag{50}$$

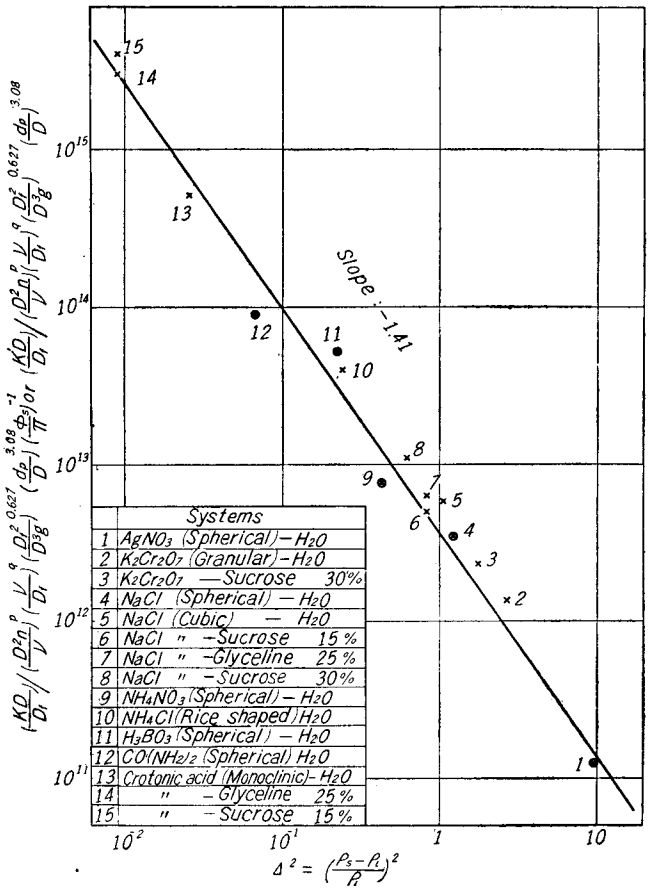

Fig. 31. $(Sh)/(Re)^p(Sc)^q(D_f^2/D^3g)^{0.627}(\delta)^{3.08}(\Phi_s/\pi)^{-1}$ *vs.* Δ^2.

When the surface shape factor Φ_s is known, the relation is expressed by,

$$\left(\frac{KD}{D_f}\right) = 3.60\times10^{12}\left(\frac{D^2n}{\nu}\right)^p\left(\frac{\nu}{D_f}\right)^q\left(\frac{D_f^2}{D^3g}\right)^{0.627}\left(\frac{d_p}{D}\right)^{3.08}\left(\frac{\rho_s-\rho_l}{\rho_l}\right)^{-2.82}\left(\frac{\Phi_s}{\pi}\right)^{-1} \tag{51}$$

where the exponents p and q are given by Eqs. (24) and (46) respectively.

Conclusions

(1) Various methods for determining the rate of solution of solid particles were tested. The results were in excellent agreement except for the case of extremely fine particles.

(2) It was found that a spherical particle dissolving in an agitated liquid always maintains its spherical shape.

(3) The mass transfer coefficient for spherical particle-liquid systems may be regarded as constant until the fraction of dissolution amounts to about 30%.

(4) As for the various shapes of solid particles, the product of the mass transfer coefficient (K) and the shape factor (α_v), is almost unchanged until the weight percent of dissolved solute reaches about 25%.

(5) The physical properties of the solid particles (*i.e.*, their density, size and shape), the viscosity and density of the liquid and the type and dimensions of the agitation apparatus, were found to be important factors controlling mass transfer in agitated liquid-solid systems.

(a) The rate of increase in dissolution velocity (or mass transfer coefficient) with increase in agitator speed "p" is a characteristic value for a given agitator and is an important criterion for planning agitation performance.

(b) The authors obtained a dimensionless equation [Eq. (24)] representing a general correlation between p and related variables.

(c) As shown by Eq. (24), the value p becomes larger with an increase in the difference in density between liquid and solid and with decrease in particle size.

The effect of the particle shape upon p is insignificant. In addition, the higher the viscosity of the liquid, the smaller the value of p, and the larger the dimensions of the agitator in a series of geometrically similar agitation systems, the larger the value of p.

(d) Hence it is inferred that the effect of the increase in the agitator speed to decrease the diffusional resistance in the diffusion film becomes negligible when the difference in density between the liquid and solid approaches zero.

(e) In a geometrically similar agitation system where the size of the solid particles is also taken to be proportional to the size factor of the system, when using the same liquid and solid a dimensionless equation (45) is given, which shows that in a series of geometrically similar systems the mass transfer coefficient is proportional to $D^{2p_2-2.88}$.

This result gives an important criterion for scaling up of the agitator for liquid-solid mass transfer.

(f) Effect of the viscosity of the agitated liquid is shown by Eqs. (46) and

(47), which show that the mass transfer coefficient (K) increases in proportion to ν^{p-q}.

(**g**) As for the effect of the size of the solid particles d_p and the difference in density between the liquid and the solid ($\rho_s-\rho_l$) upon the mass transfer coefficient, whether mass transfer is increased or decreased by an increase in d_p or ($\rho_s-\rho_l$) is not uniquely determined by each of these factors alone as shown by Eqs. (24) and (48) or by Eqs. (24) and (49).

(**h**) The mass transfer coefficient decreases with an increase in the shape factor (ϕ_s), so that the value K becomes largest in the case of a sphere under the condition where the values of the other variables are fixed [refer to Eq. (51)].

(**6**) Between the agitator speeds of N_f and N_a all the data are correlated by the dimensionless equations (50) and (51) where the exponents p and q are given by Eqs. (24) and (46) respectively.

These equations represent a general correlation of the variables involved in determining the magnitude of the rate of mass transfer in agitated liquid-solid systems, and are used to estimate mass transfer data for any liquid-solid combination in a series of dimensionally similar agitators.

Acknowledgment

The authors wish to express their appreciation to the Ministry of Education in Japan for providing scientific research aid fund No. 59390.

The spherical crystals of NaCl used in the present investigation were presented by the Nihon Senbaikosha Chuo Kenkyusho (Japan Monopoly Corporation), and the authors wish to express their heartiest appreciation to Dr. J. Sugi for this courtesy.

Spherical ammonium nitrate was presented by the Sumitomo Chemical Company Ltd. Spherical urea by the Nissan Kagaku Kogyo Co. Ltd, granular zinc by the Sawamura-aen Co. Ltd, and granular ammonium chloride by the Asahi Garasu Co. Ltd. Thanks are also due to these companies.

Notations Used

A	: total surface area of the solid particles	[cm^2]
A_0	: total surface area of the solid particles at time $\theta=0$	[cm^2]
A_s	: $\alpha_v n^{1/3} W_s^{2/3}/\rho_s^{2/3}$ [refer to Eq. (8)]	[cm^2]
b	: width of an impeller blade [refer to **Fig. 1**]	[cm]
C, C', C'', C''' and C_1	: a constant	[—]
C	: concentration of solution at time θ	[g/cm^3]

C_s : concentration of solution at saturation [g/cm³]
d : diameter of an impeller [cm]
d_p : particle diameter equivalent to that of a sphere of equivalent weight [mm]
D : diameter of the agitation vessel [cm]
D_f : diffusion coefficient of solute [cm²/sec]
f_1, F, F' F_1 and F_2 : mathematical symbols representing "function of" [—]
Fr : Froude number [—]
g : acceleration of gravity [cm/sec²]
H_l : liquid depth [cm]
H_p : elevation of the impeller above the bottom [cm]
K : mass transfer coefficient [cm/min]
$K'=K\varnothing_s/\pi$ [cm/min]
$m=W_s-W_0$ [g]
n : number of solid particles used [—]
n : agitator speed [r.p.s.]
n_p : number of impeller blades [—]
N : agitator speed [r.p.m.]
N_a : agitator speed at which suction of air occurs [r.p m.]
N_f : agitator speed at which fluidization of particles occurs [r.p.m.]
p : exponent of Reynolds number or N [—]
p_1 : exponent of Re of N in stagnant range [—]
p_2 : exponent of Re or N in fluidized range [—]
p_3 : exponent of Re or N in aerated range [—]
$p_{\Delta 0}$: exponent of Re at $\Delta=\Delta$ and $\delta=0$ [—]
$p_{\Delta\delta}$: exponent of Re at $\Delta=\Delta$ and $\delta=\delta$ [—]
Δp : pressure difference [refer to **Fig. 2**] [g/cm²]
q : exponent of Schmidt number [—]
q_0 : exponent of Schmidt number q at $\delta=0$ [—]
R : total rate of solution [g/min]
$Re=D^2n\rho_l/\mu$: modified Reynolds number [—]
$Sc=\mu/\rho_l\cdot D_f$: Schmidt number [—]
Sh : Sherwood number [—]
u : relative velocity between solid particle and liquid-bulk [cm/sec]
V : total volume of solution [cm³]
V_p : total net volume of solid particles [cm³]
$V_{p'}$: total apparent volume of solid particles [cm³]
w : weight of solid particles [g]
W : weight of solid particles at time θ [g]

W_d: weight of solid dissolved at time θ [g]
W_0: initial weight of solid particles used [g]
W_s: weight of solid particles at saturation [g]
x : thickness of effective diffusional film [cm]
x : weight fraction of dissolved solid [—]
$X = W_d/W_s$ [—]
$Y = W_0/W_s$ [—]
$Z = K\alpha_v n^{1/3} W_s^{2/3}\theta/\rho_s^{2/3} V$ [refer to Eq. (3)] [—]
α, α', β, β', γ, γ', δ, δ', ε, ε', λ, λ' and ω: a constant [—]
α_v : a shape factor relating the area and volume of a solid particle [—]
α_w : a shape factor relating area and weight of a solid particle [$cm^2/g^{2/3}$]
$\delta = d_p/D$: dimensionless ratio of particle size [—]
$\Delta = (\rho_s - \rho_l)/\rho_l$: dimensionless ratio of density difference [—]
θ : angle of impeller blades [degree]
θ : time elapsed from moment of interfacial contact [sec] or [min]
μ : viscosity of agitated liquid [c.p.]
$\nu = \mu/\rho_l$: kinematic viscosity of liquid [cm^2/sec]
ρ_l : density of agitated liquid [g/cm^3]
ρ_s : density of solid particle [g/cm^3]
$\Delta\rho$: density difference between liquid and solid [g/cm^3]
$\Phi_s = A/n d_p^2$: surface shape factor (which is π for sphere) [—]

Literature cited

1) S. Nagata, M. Adachi and I. Yamaguchi: THIS MEMOIRS.: Vol. XX, No. 1, 72 (1958).
2) R. H. Wilhelm, L. H. Conklin and T. C. Sauer: Indust. Engng. Chem., **33**, 453 (1941).
3) E. C. Bingham: "Fluidity and Plasticity," pp. 76, 1st Ed., McGraw-Hill Book Co., Inc., New York (1922).
4) A. W. Hixson and J. H. Crowell: Indust. Engng. Chem., **23**, 923 (1931).
5) S. Nagata, *et al.*: Chem. Engng. (Japan), **17**, 114 (1953).